

1 **TITLE:** Epithelial restitution defect in neonatal jejunum is rescued by juvenile mucosal
2 homogenate in a pig model of intestinal ischemic injury and repair

3
4 **AUTHORS:** Amanda L. Ziegler¹, Tiffany A. Pridgen¹, Juliana K. Mills¹, Liara M. Gonzalez¹,
5 Laurianne Van Landeghem², Jack Odle³, Anthony T. Blikslager¹

6
7 **AFFILIATIONS:** 1. Department of Clinical Sciences, College of Veterinary Medicine, NC State
8 University, Raleigh, NC, USA; 2. Department of Molecular Biomedical Sciences, College of
9 Veterinary Medicine, NC State University, Raleigh, NC, USA; 3. Department of Animal Science,
10 College of Agriculture and Life Sciences, NC State University, Raleigh, NC, USA

11
12 **RUNNING HEAD:** Rescuable intestinal repair defect in neonates

13
14 **CORRESPONDENCE:**
15 Anthony Blikslager
16 College of Veterinary Medicine
17 1060 William Moore Drive
18 Raleigh, NC 27607
19 Phone: 919-513-7725
20 Email: Anthony_Blikslager@ncsu.edu

21
22

23 **ABSTRACT**

24 Intestinal ischemic injury results sloughing of the mucosal epithelium leading to host sepsis and
25 death unless the mucosal barrier is rapidly restored. Neonatal necrotizing enterocolitis (NEC) and
26 volvulus in infants is associated with intestinal ischemia, sepsis and high mortality rates. We have
27 characterized intestinal ischemia/ repair using a highly translatable porcine model in which
28 juvenile (6-8-week-old) pigs completely and efficiently restore barrier function by way of rapid
29 epithelial restitution and tight junction re-assembly. In contrast, separate studies showed that
30 younger neonatal (2-week-old) pigs exhibited less robust recovery of barrier function, which may
31 model an important cause of high mortality rates in human infants with ischemic intestinal disease.
32 Therefore, we aimed to further refine our repair model and characterize defects in neonatal barrier
33 repair. Here we examine the defect in neonatal mucosal repair that we hypothesize is associated
34 with hypomaturity of the epithelial and subepithelial compartments. Following jejunal ischemia in
35 neonatal and juvenile pigs, injured mucosa was stripped from seromuscular layers and recovered
36 *ex vivo* while monitoring transepithelial electrical resistance (TEER) and ³H-mannitol flux as
37 measures of barrier function. While ischemia-injured juvenile mucosa restored TEER above
38 control levels, reduced flux over the recovery period and showed 93±4.7% wound closure,
39 neonates exhibited no change in TEER, increased flux, and a 11±23.3% increase in epithelial
40 wound size. Scanning electron microscopy revealed enterocytes at the wound margins of
41 neonates failed to assume the restituting phenotype seen in restituting enterocytes of juveniles.
42 To attempt rescue of injured neonatal mucosa, neonatal experiments were repeated with the
43 addition of exogenous prostaglandins during *ex vivo* recovery, *ex vivo* recovery with full thickness
44 intestine, *in vivo* recovery and direct application of injured mucosal homogenate from neonates
45 or juveniles. Neither exogenous prostaglandins, intact seromuscular intestinal layers, nor *in vivo*
46 recovery enhanced TEER or restitution in ischemia-injured neonatal mucosa. However, *ex vivo*
47 exogenous application of injured juvenile mucosal homogenate produced a significant increase
48 in TEER and enhanced histological restitution to 80±4.4% epithelial coverage in injured neonatal

49 mucosa. Thus, neonatal mucosal repair can be rescued through direct contact with the cellular
50 and non-cellular milieu of ischemia-injured mucosa from juvenile pigs. These findings support the
51 hypothesis that a defect in mucosal repair in neonates is due to immature repair mechanisms
52 within the mucosal compartment. Future studies to identify and rescue specific defects in neonatal
53 intestinal repair mechanisms will drive development of novel clinical interventions to reduce
54 mortality in infants affected by intestinal ischemic injury.

55

56 **INTRODUCTION**

57 The intestinal mucosa is lined by a single layer of epithelial cells, which form the principal barrier
58 against luminal bacteria and their toxins and simultaneously facilitate selective absorption of
59 electrolytes, water and nutrients. Intestinal ischemia leads to the breakdown of the intestinal
60 epithelial barrier and onset of sepsis (1). Therefore, rapid and complete repair of this barrier is
61 critical to patient survival following an ischemic event. Ischemic injury is an important contributor
62 to intestinal mucosal disruption and inflammation in devastating neonatal diseases such as
63 neonatal necrotizing enterocolitis (NEC), volvulus and spontaneous intestinal perforation (SIP)
64 (2). NEC occurs in preterm infants as well as term infants with congenital heart disease and is
65 associated with an estimated mortality rate between 20 and 30% (3, 4). Clinical interventions for
66 neonatal intensive care unit patients with NEC currently include supportive care, attention to
67 sepsis that results from disruption of the intestinal barrier, and ultimately intestinal resection
68 when necessary (5). Novel treatments have focused on enhancing denovo formation of new
69 epithelial cells, but this requires support of the patient for days following the initial injury until
70 newly produced epithelial cells can restore the mucosal barrier (5, 6). In this subacute repair
71 phase, remaining epithelium must immediately reconstitute the damaged barrier to curtail sepsis
72 early and prevent host mortality until the regenerative phase can fully restore intestinal
73 architecture (1). For this reason, our lab has focused on understanding the mechanisms of the

74 subacute phase of repair, as interventions enhancing this phase will improve patient survival
75 and hopefully reduce the need for resection in order to improve long-term quality of life.

76 Our lab studies mechanisms of subacute mucosal repair following ischemia using a
77 porcine model because the pig has many fundamental anatomical, physiological, immunological
78 and nutritional similarities to humans, and therefore provides a powerful translational model of
79 human digestive disease, including ischemia (7-15). In juvenile (6-8-weeks-old) pigs, we have
80 shown rapid repair of ischemia-injured mucosa involving contraction of denuded villi, epithelial
81 cell migration across the denuded basement membrane (restitution), and re-assembly of tight
82 junctions, resulting in swift recovery of intestinal barrier function (1, 15). Alternatively, we noted
83 that in our studies of neonatal (2-week-old) pigs, barrier function failed to recover as efficiently
84 following ischemic injury as compared to studies with juvenile aged pigs (16, 17). An immaturity-
85 related defect in epithelial repair may be an important contributor to the high morbidity and
86 mortality seen in infants affected by intestinal ischemia and barrier injury. For this reason,
87 understanding specific rescuable defects in subacute intestinal repair mechanisms in immature
88 patients may expedite development of novel clinical interventions to reduce mortality in infants
89 affected by intestinal ischemic injury. Therefore, we aimed to further refine our repair model and
90 identify rescuable defects in neonatal barrier repair. Here we describe a defect in mucosal repair
91 in neonates that we propose is associated with insufficient pro-reparative signals from a
92 hypomature mucosal compartment. In support of this, we demonstrate that exogenous
93 application of injured mucosal homogenate of older animals can rescue subacute repair of
94 injured neonatal tissue.

95

96 **METHODS**

97 ***Experimental Surgery.*** All procedures were approved by NC State University Institutional
98 Animal Care and Use Committee. Two-week-old and 6-8-week-old Yorkshire cross pigs of
99 either sex were sedated using xylazine (1.5 mg/kg) and ketamine (11 mg/kg). Anesthesia was

100 induced with isoflurane vaporized in 100% oxygen via face mask, after which pigs were
101 orotracheally intubated for continued delivery of isoflurane to maintain general anesthesia. Pigs
102 were placed on a water-circulated heating pad and intravenous fluids were administered at a
103 maintenance rate of $15 \text{ ml} \cdot \text{kg}^{-1} \cdot \text{h}^{-1}$ throughout surgery. The distal jejunum was accessed via
104 midline or paralumbar incision and 8-10 cm loops were ligated in segments and subjected to 30,
105 45-, 60-, and 120-minutes of ischemia via ligation of local mesenteric blood vessels with 2-0
106 braided silk suture, bulldog clamps, or hemostats. After ischemia, tissues were reperfused for *in*
107 *vivo* recovery or loops were removed and placed in oxygenated (95% O₂/ 5% CO₂) Ringers
108 solution for *ex vivo* recovery. Additional loops not subjected to ischemia were used as control
109 tissue. At the time of loop resection, pigs were euthanized with an overdose of pentobarbital.
110 **Ussing chamber studies.** In experiments where mucosa was stripped, the outer seromuscular
111 layers were removed by dissection in oxygenated Ringers solution. For full thickness recovery
112 studies, the mucosal tissue was left intact with the seromuscular layer. For *ex vivo* recovery,
113 jejunal tissue was mounted in 1.12 cm² aperture Ussing chambers. The tissues were bathed in
114 10 ml warmed oxygenated (95% O₂/ 5% CO₂) Ringer solution on the serosal and mucosal
115 sides. Serosal Ringer solution also contained 10mM glucose while the mucosal Ringers solution
116 was osmotically balanced with 10mM mannitol. Bathing solutions were circulated in water-
117 jacketed reservoirs and maintained at 37°C. The spontaneous potential difference (PD) was
118 measured using Ringer-agar bridges connected to calomel electrodes, and the PD was short-
119 circuited through Ag-AgCl electrodes with a voltage clamp that corrected for fluid resistance.
120 Resistance ($\Omega \cdot \text{cm}^2$) was calculated from spontaneous PD and short-circuit current (I_{sc}). If the
121 spontaneous PD was between -1 and 1 mV, the tissues were current-clamped at $\pm 100 \mu\text{A}$ and
122 the PD re-recorded. I_{sc} and PD were recorded every 15-minutes for 120-minutes. From these
123 measurements, TEER is calculated. For exogenous prostaglandin experiments, 1 μM 16,16-
124 dimethylprostaglandin E₂ was added to the basolateral chamber after the 15-minute reading for

125 the remainder of recovery. To measure prostaglandin E₂ production by the tissues, samples of
126 Ringers solution were taken from the basolateral chamber to be assayed with a prostaglandin
127 E₂ metabolite ELISA kit (Cayman Chemical, catalog #514531, Ann Arbor, MI, USA). To assess
128 barrier integrity in mucosa recovered *in vivo*, tissues were mounted on Ussing chambers in the
129 same way but for only 60-minutes and five resistance measurements were averaged.

130 **Isotopic mannitol flux studies.** All fluxes were conducted under short-circuit conditions (tissue
131 clamped to 0 mV). ³H-mannitol (0.2 µCi/ml diluted in 10mM mannitol) was placed on the
132 mucosal side of tissues. During *ex vivo* recovery experiments, two 60-minute fluxes from 0- to
133 60-minutes and from 60- to 120-minutes of the experimental recovery period by taking samples
134 from the opposite side of that of isotope addition and counted for ³H β-emission in a scintillation
135 counter. Mucosal-to-serosal fluxes (J_{ms}) of mannitol were calculated using standard
136 equations.(18) To assess barrier integrity in mucosa recovered *in vivo*, a single 60-minute flux
137 was performed.

138 **Mucosal Homogenate and Supernatant.** To obtain mucosal homogenates for *ex vivo* rescue
139 experiments, 30-minute ischemia-injured jejunum from neonatal and juvenile pigs was
140 harvested at the same time as tissues intended for *ex vivo* recovery. The mucosa was scraped
141 from the jejunum using glass slides and collected into conical tubes at a ratio of 1 gram of tissue
142 per 1ml of Ringers solution for 20-30 seconds of homogenization with a handheld tissue
143 homogenizer (Omni International Inc., Kennesaw, GA, USA). Homogenate was then diluted to
144 an experimental concentration of 0.2g/ml in Ringers solution, which was the highest
145 concentration that would freely circulate through the chambers. To generate the supernatant,
146 tubes were centrifuged at 5,400 RCF for 5-minutes and only the top layer free of solids was
147 used. Recovery experiments began under standard protocols with Ringers solution. After the 0-
148 and 15-minute electrical readings were recorded, the apical and/ or basolateral Ringers was
149 drained and either the homogenates or supernatants were placed in the reservoirs, bathing the

150 recovering neonatal mucosa from one or both sides. Glucose and mannitol were added to the
151 homogenate or supernatant at standard concentrations.

152 **Light microscopy and histomorphometry.** Tissues were fixed for 18 hours in 10% formalin at
153 room temperature or 4% paraformaldehyde (PFA) in phosphate-buffered saline (PBS) at 4°C
154 immediately following ischemic injury or after 120-minutes *ex vivo* recovery period. Formalin-
155 fixed tissues were transferred to 70% ethanol and then paraffin-embedded, sectioned (5µm) and
156 stained with hematoxylin and eosin for histomorphological analysis. For morphometric analysis
157 of villus injury, the base of the villus was defined as the opening of the neck of the crypts and
158 height of epithelialization, total height and width of villus were measured using NIH Image J®
159 Software. The surface area of the villus was calculated as previously described using the
160 formula for the surface area of a cylinder modified by subtracting the base of the cylinder and
161 adding a factor that accounted for the hemispherical shape of the villus tip(18). The percentage
162 of villus epithelialization was used as an index of epithelial restitution.

163 **Immunofluorescence histology.** PFA-fixed tissues were transferred to 10% sucrose, then
164 30% sucrose in PBS for 24 hours each for cryopreservation. The tissues were then embedded
165 in optimal cutting temperature (OCT) compound and sectioned (7µm) onto positively charged
166 glass slides for immunostaining. Slides were washed 3 times in PBS to rehydrate the tissue and
167 remove OCT compound and were treated for antigen retrieval by in a decloaking chamber for
168 30 seconds at 120°C followed by 90°C for 10 seconds in a reveal decloaker solution (Biocare
169 Medical, Concord, CA, USA). Tissues were cooled for 20-minutes at room temperature then
170 places in PBS-0.3% Triton -100 solution for 20-minutes to permeabilize the tissues. Tissues
171 were washed twice in PBS and incubated in blocking solution (Dako, Carpinteria, CA, USA) for
172 1 hour at room temperature. To mark the basement membrane, tissues were incubated in
173 polyclonal rabbit anti-collagen IV IgG (Abcam, Cambridge, MA, USA; Catalog #ab6586) at a
174 dilution of 1:200 in antibody diluent (Dako, Carpinteria, CA, USA) overnight at 4°C. To mark the
175 brush border of villus enterocytes, tissues were incubated in polyclonal goat anti-villin (Santa

176 Cruz Biotechnology, Dallas, TX, USA; catalog #sc-7672) at a dilution of 1:500 in antibody
177 diluent (Dako, Carpinteria, CA, USA) overnight at 4°C. Intestinal fatty acid binding protein
178 (iFABP), expressed in the cytoplasm of mature enterocytes and known to leak out during
179 ischemic injury (19, 20), was also labeled by incubating in polyclonal goat anti-iFABP (Abcam,
180 catalog #ab60272) at a dilution of 1:200 in antibody diluent (Dako, Carpinteria, CA, USA)
181 overnight at 4°C. Tissues were placed in donkey anti-rabbit IgG conjugated to Alexa Fluor 568
182 (Invitrogen, catalog #A10042) or donkey anti-goat IgG conjugated to Alexa Fluor 488
183 (Invitrogen, product #A11055) at a dilution of 1:500 in antibody diluent for 1 hour at room
184 temperature. Tissues were counterstained with nuclear stain 4',6-Diamidino-2-Phenylindol
185 (DAPI, Invitrogen, catalog #D1306) diluted 1:1000 in antibody diluent for 5 minutes at room
186 temperature. Images were captured using an inverted fluorescence microscope (Olympus IX81,
187 Tokyo, Japan) with a digital camera (ORCA-flash 4.0, Hamamatsu, Japan) using 10X objective
188 lens with numerical aperture of 0.3 (LUC Plan FLN, Olympus, Tokyo, Japan). Specificity of
189 primary antibodies and lack of non-specific secondary antibody binding were confirmed by
190 secondary only negative controls.

191 **Scanning electron microscopy.** 30-minute ischemic neonate and juvenile jejunum were fixed
192 at 0-, 30- and 120-minutes during the experimental recovery period in separate experiments.
193 Mucosa was rinsed briefly with PBS to remove surface debris followed by immersion fixation in
194 2% paraformaldehyde/2.5% glutaraldehyde/0.15M sodium phosphate buffer, pH 7.4. Specimens
195 were stored in the fixative overnight to several days at 4°C before processing for SEM
196 (Microscopy Services Laboratory, Dept. of Pathology and Laboratory Medicine, UNC, Chapel
197 Hill, NC, USA). After three washes with 0.15M sodium phosphate buffer (PBS), pH 7.4, the
198 samples were post-fixed in 1% osmium tetroxide in PBS for 1-hour and washed in deionized
199 water. The samples were dehydrated in ethanol (30%, 50%, 75%, 100%, 100%), transferred to
200 a Samdri-795 critical point dryer and dried using carbon dioxide as the transitional solvent
201 (Tousimis Research Corporation, Rockville, MD). Tissues were mounted on aluminum

202 planchets using silver paste and coated with 15nm of gold-palladium alloy (60Au:40Pd, Hummer
203 X Sputter Coater, Anatech USA, Union City, CA). Images were taken using a Zeiss Supra 25
204 FESEM operating at 5kV, using the SE2 detector, 30 μ m aperture, and a working distance of 10
205 to 12mm (Carl Zeiss Microscopy, LLC, Peabody, MA).

206 **Statistical Analysis.** All data was analyzed using SigmaPlot[®] (Systat[®]; San Jose, California,
207 USA) and Prism[®] (GraphPad[®]; La Jolla, California, USA) statistical software. Data were
208 reported as means \pm SE for a given number (n) of animals for each experiment. Results were
209 analyzed by student's t-test, or two- or three- way ANOVA on repeated measures. For analyses
210 where significance was detected by ANOVA, Tukey's test or Sidak's test was utilized for post
211 hoc pairwise multiple comparisons. The α -level for statistical significance was set at $P < 0.05$.
212 Where a significant time by treatment interaction was found, a one-way ANOVA was performed
213 to identify individual treatment effects.

214

215 **RESULTS**

216 **Ischemia induces time-dependent injury that is similar in neonatal and juvenile pigs**

217 In order to determine the effect of postnatal age on level of injury following intestinal ischemia,
218 neonatal and juvenile aged animals were subjected to jejunal ischemia for varying durations and
219 intestinal barrier integrity was studied. In both neonatal and juvenile jejunum, 30-, 45-, 60-, and
220 120-minutes of ischemia induced villus contraction (Fig. 1A) and time-dependent epithelial injury
221 (Fig. 1B). As expected, increasing durations of ischemia led to increasing injury (decreasing
222 epithelial coverage), and there was a significant reduction in villus height after recovery in both
223 neonates and juveniles (Fig. 1A). However, there was no significant difference in injury between
224 neonates and juveniles within each injury duration when measured as percent epithelial
225 coverage (fig. 1B).

226 To further characterize the degree of mucosal injury induced by 30-minutes ischemia in
227 the two age groups, fixed-frozen sections were immunolabeled for enterocyte and extracellular

228 matrix markers. Villin, which shows a strong immunoreactivity in the brush border of mature
229 enterocytes on the villi, and collagen IV, the primary matrix component of the basement
230 membrane, were probed in control and ischemic mucosa from both neonates and juveniles.
231 Both age groups showed similar disruption of the enterocyte brush border due to epithelial
232 sloughing restricted mainly to the villus tips (fig. 2A, green). A continuous lining of collagen IV at
233 the denuded surfaces of the villus tips indicates that there was no loss of subepithelial tissue
234 due fracturing of the villi during ischemic injury in either the neonate or juvenile mucosa (fig. 2A,
235 red). As a marker of mature enterocyte cytoplasm as well as a functional marker of intestinal
236 ischemic injury(19, 20), iFABP was also probed. The iFABP signal was restricted to the
237 cytoplasm of enterocytes and was more highly expressed towards the villus tips in both age
238 groups. Wound-adjacent enterocytes expressed iFABP in both neonates and juveniles (fig. 2B).

239

240 **Failure of *ex vivo* barrier repair in neonates is due to a defect in restitution**

241 We next wanted to determine if there was a difference in the ability of neonatal and juvenile
242 tissues to repair, as suggested by our previous studies (16, 17). Mucosal tissues were stripped
243 from the seromuscular layers in preparation for *ex vivo* recovery in Ussing chambers. At the
244 beginning of *ex vivo* recovery, all injured tissues of both age groups demonstrated reduced
245 TEER as compared to age-matched controls (Fig. 3A). In juvenile tissues, TEER increased to
246 the level of control tissues in both the 45- and 60-minute-injured groups, and the 30-minute-
247 injured group exceeded the control levels during the 120-minute *ex vivo* recovery period.
248 Tissues injured by 120-minutes ischemia increased but did not meet control TEER levels during
249 recovery (Fig. 3A, right panel). In neonatal tissues, there was no change in TEER throughout
250 the entire *ex vivo* recovery period regardless of duration of ischemic injury (Fig. 3A, left panel).
251 The most notable differences between neonates and juvenile animals were seen when
252 comparing the 30-minute injured jejunum, where there was a significant difference in TEER of
253 juvenile tissues after 90-minutes of recovery versus neonatal tissues (Fig. 3B). This was

254 accompanied by a decrease in ^3H -mannitol flux from the first hour to the second hour of the
255 recovery period in juveniles as compared to no change in neonates (Fig. 3C). Histology
256 revealed a remaining defect in the intestinal epithelium at the villus tips following recovery of
257 injured neonatal jejunum as compared to a 'macroscopically sealed' layer of newly restituted
258 epithelium at the villus tips in juveniles (Fig. 3D). In 30-minute ischemia injured tissues,
259 histomorphometry quantified 93% wound closure in juveniles as compared to an 11% increase
260 in wound size in neonates following recovery (Fig. 3E). Due to the notable differences in barrier
261 recovery in juveniles versus neonates following 30-minutes ischemia, all studies that follow
262 utilized 30-minutes of jejunal ischemia.

263

264 **Neonatal wound-associated epithelial cells fail to assume a migratory phenotype**

265 Based on the lack of restitution noted, we next wanted to assess the nature of the wound-
266 adjacent enterocytes more closely to determine whether these cells were undergoing
267 phenotypic changes associated with epithelial restitution. To do this, ischemia-injured villus tips
268 undergoing *ex vivo* recovery were visualized by scanning electron microscopy. Initially after
269 injury, both neonate and juvenile mucosa exhibited damaged and sloughing enterocytes at the
270 villus tips. Contrasting to the juvenile shorter villi, the longer neonatal villi formed concentric
271 folds in the intact epithelium indicative of the contraction of the villus core beneath the surface
272 (Fig. 4A). In juvenile tissues, enterocytes at the defect margins assumed a migratory phenotype
273 characterized by the depolarization/ flattening of the cells, loss of microvilli, and extension of
274 lamellipodia into the wound bed (Fig. 4B, right panels). Interestingly, in neonatal tissues, the
275 cells assumed an atypical spherical shape (Fig. 3B, left panels) which to our knowledge has not
276 been reported before. These spherical cells did not appear to assist wound closure, but rather
277 remained at the edges of the wound. Indeed, in contrast to juvenile tissues, enterocytes beside
278 the wound bed retained a polarized phenotype with no evidence of assuming any of the features

279 of restitution. More specifically, they did not flatten, retained microvilli, and lacked the
280 lamellipodial extensions indicative of cell crawling.

281

282 **Neither a PGE₂ treatment, the presence of the subepithelial compartment during *ex vivo***
283 **recovery nor *in vivo* recovery rescue neonatal restitution**

284 Given the role of prostaglandins in driving villus contraction and tight junction restoration during
285 subacute repair, we wondered whether the exogenous addition of prostaglandins during *ex vivo*
286 recovery could support the restitution phase as well (1). To test this, 16,16 dimethyl-
287 prostaglandin E₂ was added to the Ringer's solution in the basolateral reservoir bathing
288 recovering neonatal tissue. Despite the addition of exogenous prostaglandin E₂, there was a
289 persistent 32±13.2% epithelial defect (Fig. 5 A, B). This resulted in no change in TEER (data not
290 shown; P>0.05 for effect of recovery on TEER by two-way ANOVA) and no change in ³H-
291 mannitol flux from the beginning to the end of the *ex vivo* recovery period (data not shown;
292 P>0.05 by Sidak's multiple comparisons test after one-way ANOVA). Additionally, endogenous
293 production of prostaglandin E₂ by recovering neonatal and juvenile mucosa during *ex vivo*
294 recovery was measured and found to be similar across age groups (Fig. S1).

295 To test whether the defect in epithelial restitution in neonatal tissues related to the lack
296 of the seromuscular layers of the jejunum (and potential signals from these layers), neonatal
297 experiments were repeated without separating the mucosa from the layers below prior to *ex vivo*
298 recovery. Histomorphometry identified a 70±6.3% epithelial coverage defect from ischemic
299 injury that persisted after full thickness *ex vivo* recovery (Fig. 5 C, D). This resulted in no change
300 in TEER (data not shown; P>0.05 for effect of recovery on TEER by two-way ANOVA) and no
301 change in ³H-mannitol flux from the beginning to the end of the *ex vivo* recovery period (data not
302 shown; P>0.05 by Sidak's multiple comparisons test after one-way ANOVA).

303 To further assess if the lack of recovery could be rescued with an intact mesenteric
304 circulation, the ischemia/ recovery experiment was repeated with vascular clamps to reverse

305 ischemia and reperfuse to recover the tissue *in vivo*. However, *in vivo* recovery resulted in
306 similar TEER and ³H-mannitol flux in the ischemic and ischemic/ *in vivo* recovered tissues (data
307 not shown, P>0.05 by one-way ANOVA for both analyses). Histomorphometry revealed a
308 50±7.4% and 56±6.6% epithelial coverage defect in ischemic and ischemic/ *in vivo* recovered
309 tissues respectively (Fig. 5 E, F).

310

311 **Mucosal homogenate from ischemia-injured juvenile jejunum rescues neonatal repair**

312 We hypothesized that the lack of recovery in neonatal tissues resulted from a lack of maturity of
313 signaling elements within the mucosal compartment. To test this hypothesis, injured neonatal
314 mucosal was recovered *ex vivo* in the presence of homogenized mucosal scrapings from 30-
315 minute ischemia-injured juvenile versus neonatal jejunum. As expected, exogenous application
316 of homogenized mucosa from injured neonatal jejunum failed to induce repair as per TEER
317 measurements (Fig. 6A). However, application of homogenized mucosa from injured juvenile
318 jejunum to both sides of the recovering neonatal tissue induced a robust increase in TEER in
319 injured neonatal mucosa (Fig. 6A). Interestingly, application to either the basolateral or the
320 apical side of the tissue did not induce any changes in the TEER (Fig. 6A). We then examined
321 histological specimens prior to and following recovery to see if changes in TEER were
322 associated with changes in epithelial coverage. This revealed an increase in epithelial restitution
323 in injured neonatal tissues recovered in the presence of injured juvenile mucosal homogenate
324 when applied both apically and basolaterally (Fig. 6 B, C). In contrast, application to either the
325 basolateral or the apical side of the tissue, or the application of homogenized mucosa from
326 injured neonatal jejunum did not produce the same effect. Histomorphometry indicated that
327 tissues restituted to 80±4.4% epithelial coverage when exposed on both sides to the juvenile
328 homogenate as compared to 40-60% in all other groups. Finally, to test whether the
329 components within the injured juvenile homogenate responsible for inducing repair were soluble
330 factors, the mucosal homogenates were centrifuged at 5,400 RCF and only the supernatant was

331 applied to both sides of recovering neonatal mucosa *ex vivo*. Application of neonatal or juvenile
332 supernatants produced no effect on TEER during 120-minutes *ex vivo* recovery (Fig. 7A). This
333 was associated with no difference in epithelial coverage versus untreated tissue; there were
334 persistent defects in restitution in all groups (Fig. 7 B, C).

335

336 **DISCUSSION**

337 NEC, volvulus and SIP are associated with mucosal disruption and inflammation due in part to
338 intestinal ischemia (2). NEC is associated with estimated mortality rates between 20 and 30%,
339 with the highest rates in neonates requiring surgery to resect intestine that fails to recover from
340 injury (3, 4). In the subacute repair phase, epithelium adjacent to areas of wounding has been
341 shown in animal models to efficiently restore barrier function by way of villus contraction,
342 epithelial restitution, and tight junction restoration to limit sepsis, preserve intestinal viability and
343 reduce host morbidity and mortality (1). However, in the present study, we have shown that
344 there is a marked defect in the degree to which epithelial cells in neonatal pigs are able to
345 reconstitute, and this is interestingly not the case in sow-matched piglets 6-weeks-of-age, which are
346 only 4-weeks older. For example, quantifying restitution by histomorphometry following 30-
347 minutes of ischemia in the two age groups revealed a stark difference in the percent wound
348 closure between neonates (-11%) and juveniles (93%). Furthermore, juvenile animals
349 demonstrate complete epithelial restitution and barrier restoration (as measured by TEER and
350 ³H-mannitol flux) in tissues injured with up to 60-minutes ischemia and do this in a remarkably
351 short period of *ex vivo* recovery (120-minutes). This complete barrier restoration following
352 ischemic injury in our juvenile pig model is consistent with similar studies in the small intestine of
353 adult human patients (19, 21). The disparity in repair between neonates and juvenile animals
354 may partly explain high mortality rates associated with intestinal ischemic disease in infants.

355 One possibility that we considered to explain poor reparative responses in neonates in
356 this study is that the neonatal mucosa may be time-dependently more susceptible to ischemic

357 damage. One reason to consider this is the elongated height of villi in neonates, which would
358 theoretically increase the counter-current exchange of oxygen within the villus vasculature that
359 exacerbates ischemic injury at the tips of the villi(1, 22). However, we were able to show that
360 intestinal ischemia induces a similar degree of injury to the epithelium of both neonates and
361 juveniles, relative to total villus length, as per our data demonstrating no significant difference in
362 ischemia-induced loss of epithelial coverage in juvenile versus neonatal tissues. Furthermore,
363 epithelial sloughing was shown to be restricted to the villus tips and the affected cells are mainly
364 villin- and iFABP-expressing cells, indicating the injured cell population in both neonates and
365 juvenile animals is composed of mostly differentiated enterocytes (20, 23). An important aspect
366 of repair is villus contraction, which we thought might pose a significant challenge in neonates
367 with such longer villi. However, neonatal villi undergo substantial contraction during recovery as
368 evidenced by marked shortening of villus length by histomorphometry, creasing of the remaining
369 epithelium as the villus core contracts on SEM, and an intact basement membrane on
370 immunohistochemistry indicating there is no breakage of the subepithelial villus core.

371 The basement membrane was of added interest to us because of the critical role this
372 plays in signaling and facilitating cell crawling. We examined the basement membrane of the
373 wounded villi by labeling with collagen IV and appeared to be continuous and intact in both age
374 groups. A defect in the basement membrane is thus likely not responsible for the impaired
375 epithelial crawling noted in neonates. However, we did not examine any differences in the
376 composition of other basement membrane constituents (nidogen, sulfated proteoglycans, and
377 laminins) between neonates and juveniles. Notably, laminin isoforms, which are differentially
378 expressed and often developmentally regulated, have differing regulatory properties for cell
379 adhesion and migration and may be of interest for future study (24, 25).

380 Focusing specifically on epithelial crawling during restitution, enterocytes bordering the
381 wound bed must depolarize and form lamellipodia to spread into and migrate across the defect
382 until they contact other migrating epithelial cells, effectively closing the defect(1). We visualized

383 this phenotype in recovering juvenile mucosa by SEM. More specifically, juvenile enterocytes at
384 the wound margins could be seen assuming a migratory phenotype, flattening and spreading
385 the redundant membrane of their microvilli into lamellipodia into the wound bed to close the
386 defect. This was in marked contrast to the wound-adjacent enterocytes of neonates, which
387 remained tall and round with intact microvilli, showing no evidence of spreading and lamellipodia
388 formation. In addition, these cells did not appear columnar either, but rather appeared to have
389 taken on a spherical brush-border-covered 'tennis ball'-like appearance that suggested some
390 level of cellular dysfunction. These findings suggest that neonatal enterocytes lack a
391 mechanism of epithelial migration which may include the signals from the extracellular
392 microenvironment, the appropriate receptors signal transduction pathways within the epithelium,
393 the cellular machinery required for depolarization and directional migration, or the physical
394 microenvironment required for adhesion and migration such as extracellular matrix or mucous
395 layer components.

396 Previous work by our lab has implicated prostaglandin E₂ in signaling for barrier repair in
397 the context of first and last phases of subacute repair: villus contraction and tight junction
398 reassembly(1, 26, 27). We therefore wondered if prostaglandin E₂ also played a role in inducing
399 epithelial restitution. However, ischemia-injured neonatal tissue treated with exogenous 16,16-
400 dimethylprostaglandin E₂ did not show improved recovery, and when this eicosanoid was
401 measured in the apical Ringer's solution sampled during *ex vivo* recovery, the levels detected
402 did not differ between neonatal and juvenile pigs. Therefore, prostaglandin E₂ does not appear
403 to be a key missing factor responsible for the restitution defect in neonates.

404 This repair model employs *ex vivo* recovery and stripping of the seromuscular layers
405 from the mucosa before mounting on the Ussing chambers, necessitating that the mucosa
406 recovers independently of host input from any tissue beyond the muscularis mucosa. While this
407 is not an impediment for the juvenile-aged animals, we wondered whether the addition of these
408 host signals may rescue the failed restitution in the neonates. Therefore, we repeated the

409 experiments in neonates without stripping the seromuscular layers for *ex vivo* recovery,
410 reasoning that although this maneuver is intended to reduce the thickness of tissue which must
411 be oxygenated and supplied with glucose *ex vivo*, neonatal tissues are thinner, and may be
412 more likely to repair under full thickness conditions. However, there was no enhancement of the
413 reparative response noted. In additional experiments, we took this idea a step further by
414 reperfusing neonatal tissue for 120-minutes *in vivo* in order to allow potential factors from the
415 systemic circulation and innervation to aid recovery, and to leave the tissue that much more
416 intact to enable more physiological responses to injury. However, this experimental design also
417 did not result in any notable improvement in mucosal repair and recovery of barrier function.
418 Collectively, these data suggest that there is not a component of repair signaling deep to the
419 muscularis mucosa, such as the host immune, nervous, or circulatory systems, that can rescue
420 subacute repair in injured mucosal epithelium within neonatal animals. Importantly, these
421 findings also confirm that the lack of recovery in neonatal mucosa *ex vivo* is not an artifact of the
422 experimental conditions. Indeed, our model mirrors *in vivo* pathophysiology and is therefore a
423 very powerful tool to study the development of neonatal intestinal repair mechanisms.

424 In light of systemic neonatal host inputs failing to rescue neonatal repair, we reasoned
425 that the mucosal microenvironment from animals of the older age group might contain the
426 elements required to promote repair. Indeed, this appeared to be the case because when
427 exogenous homogenized mucosal scrapings from ischemia-injured jejunum from juveniles was
428 placed in the Ussing chambers with ischemic-injured neonatal tissues, there was a robust
429 recovery of TEER and a measurable increase in epithelial restitution in the neonatal mucosa.
430 Importantly, this was not the case following application of homogenized mucosa from ischemia-
431 injured neonatal jejunum, further supporting the presence of age-dependent pro-reparative
432 factors within the juvenile milieu. These mucosal mixtures contain briefly homogenized mucosal
433 scrapings consisting of everything from the level of the muscularis mucosa to the luminal
434 surface including the live cells, cell secretory products, extracellular matrix and, very likely, the

435 adherent mucous layer and microbiota. An interesting finding was that the homogenate had to
436 be placed on both sides of recovering tissue to induce the restitution response. This may be due
437 to a dose-response effect and application on both sides provides twice the dose of the key pro-
438 repair factors. Alternatively, it may be that the key factors must act on both the basolateral and
439 apical sides to induce a response, perhaps by acting on specific membrane-bound receptors on
440 the epithelial cell, for example. Another interesting factor was that a low speed centrifugation to
441 remove all solids from the juvenile homogenate attenuated the reparative effect of the
442 homogenized mucosa, suggesting that the responsible components of the mixture either exist
443 within the solids or are a labile secretory factor needing to be continually produced by live cells
444 within the Ussing chamber reservoirs.

445 Future studies to identify the key factors responsible for producing the rescue effect in
446 these experiments will further refine our mucosal repair model to encompass the postnatal
447 development of restitution mechanisms. Paracellular signals from the lamina propria are known
448 to modulate epithelial cell functions in homeostasis and disease states and cell populations
449 within the subepithelial microenvironment are known to play a role in epithelial barrier repair
450 signaling. For example, a growing body of evidence indicates that enteric glial cells (EGC) play
451 a pivotal role in promoting intestinal epithelial repair and barrier function through the release of
452 paracrine factors such as glial-derived neurotrophic factor, pro-epidermal growth factor, 11β
453 prostaglandin $F_{2\alpha}$, and S-nitrosoglutathione (28-31). These EGC form a dense network in the
454 lamina propria in close proximity to intestinal epithelial cells, and of particular interest, the EGC
455 network of rodents has been shown to continue development after birth, with final maturation
456 completing during the postnatal period (32-34). These features may implicate the EGC network
457 in this neonatal repair defect. Key future experiments will examine the presence and role of
458 glial-derived signaling in the defects of barrier repair in neonates. A differential transcriptome
459 analysis of the juvenile and neonatal mucosal homogenate before and after ischemic injury can

460 be expected to provide valuable insight to guide future work toward key signaling mechanisms
461 and should be the next step in this line of work.

462 In conclusion, these studies show that there is a critical, but rescuable, defect in
463 epithelial restitution following ischemic injury due to age-related insufficiency of repair
464 mechanisms within the mucosal compartment. These findings may be of significant translational
465 relevance to high morbidity and mortality in pre-term and term infants afflicted with ischemia-
466 related intestinal disease. This defect may also be relevant to other mechanisms of intestinal
467 epithelial injury, expanding its applicability in numerous other intestinal diseases of neonates.
468 Identifying the specific rescuable defects in repair mechanisms will enhance our understanding
469 of the development of barrier repair mechanisms in the postnatal period and will guide future
470 clinical interventions to improve outcomes in affected infants.

471

472 **ACKNOWLEDGEMENTS**

473 The authors want to thank Gwendolyn Carnighan, Erik Wegner-Clemens, Megan Gallagher for
474 their assistance with experimental procedures and data analysis, the staff and faculty of Lab
475 Animal Resources and the Central Procedures Laboratory at NC State College of Veterinary
476 Medicine for their excellent animal care and assistance with surgical procedures, the NC State
477 Swine Educational Unit for their logistical support and exceptional animal care, and Victoria
478 Madden and Kristen White for providing their expertise in electron microscopy.

479

480 **AUTHOR CONTRIBUTIONS**

481 Conceived and designed all experiments: ALZ, ATB, LVL, JO. Performed the experiments: ALZ,
482 TAP, JKM, LMG, ATB. Contributed materials, equipment and analysis tools: JO, LMG, LVL,
483 ATB. Prepared the final manuscript: ALZ, ATB.

484

485 **FIGURES**

486 **Figure 1. Villi show similar morphometric changes following ischemic injury in neonates**
487 **and juveniles.** (A) Villus height decreases following injury and the villi shorten further following
488 120-minutes *ex vivo* recovery in both neonates and juveniles (Significant effect of recovery and
489 injury duration on villus height by two-way ANOVA in neonates, $P < 0.05$; significant effect of
490 recovery on villus height by two-way ANOVA in juveniles, $P < 0.05$). (B) Histomorphometry
491 quantified a similar decrease in epithelialization (increase in injury) with increasing durations of
492 ischemia in both age groups (significant effect of ischemia on epithelialization by two-way
493 ANOVA, $P < 0.0001$, no significant differences between age groups at each duration of injury
494 following Sidak's multiple comparisons test).

495
496 **Figure 2. Ischemia induced similar epithelial injury in both age groups.** (A) Fixed-frozen
497 sections of neonate (top rows) and juvenile (bottom rows) jejunal mucosa was probed for
498 Collagen IV (red), a component of the basement membrane, and villin (green), as a marker of
499 the brush border of mature villus enterocytes. Note that ischemia-induced enterocyte loss is
500 restricted to mainly the villus tips (white arrows), and that the basement membrane is intact in
501 the injured mucosa from both age groups (representative fields from $n=3$ per group, Scale bars
502 100 μm). (B) iFABP (green) was restricted to the cytoplasm of enterocytes with increased
503 expression toward the villus tips in both age groups. Note that wound-adjacent enterocytes
504 (white arrows) express iFABP in injured villi from both neonate and juveniles (representative
505 fields from $n=3$ per group, Scale bars 100 μm)

506
507 **Figure 3. Neonates fail to recover barrier function *ex vivo* following ischemia due to**
508 **failure of restitution.** (A) TEER over 120-minutes *ex vivo* recovery in Ussing chambers. Note
509 the return of TEER beyond control values in the 30-, 45-, and 60-minute ischemia-injured
510 juvenile mucosa within 120-minutes of *ex vivo* recovery, while the all ischemia-injured neonatal

511 tissues fail to recover TEER within 120-minutes (n=5-17, significant interaction between
512 recovery and age on three-way repeated measures ANOVA, $P \leq 0.001$). (B) TEER of 30-min
513 ischemia-injured tissues versus controls over 120-minutes *ex vivo* recovery (two-way ANOVA
514 with Sidak's multiple comparisons test, $*P \leq 0.05$, $**P \leq 0.01$). (C) Change in ^3H -mannitol flux
515 relative to controls in 30-min ischemia-injured tissues over the *ex vivo* recovery period. Note no
516 change in small molecular flux in neonates whereas juvenile tissue flux decreases from the
517 beginning to the end of the recovery period (n=6, Student's t-test, $*P \leq 0.01$). (D) Representative
518 histology shows the remaining defect in the 30-minute ischemia-injured mucosal epithelium at
519 the villus tips in neonates after recovery as compared to the restituted epithelium (arrowheads)
520 of the juvenile villi (scale bar 100 μm). (E) Histomorphometry quantified a $93 \pm 4.7\%$ wound
521 closure in juveniles as compared to a $11 \pm 23.3\%$ increase in wound size in neonates (n=6-18,
522 $*P \leq 0.05$, student's t-test).

523

524 **Figure 4. Scanning electron microscopy shows neonatal wound-associated enterocytes**
525 **fail to assume migratory phenotype seen in juveniles.** (A) Neonate and juvenile villi
526 following 30-minutes ischemia. Note the sloughing enterocytes at the tip of both villi (asterisks),
527 and the concentric folds indicating contraction of the villus core and bunching of the surface
528 epithelium in the neonate (representative of n=3, 1,000x, scale bar 30 μm) (B) Neonate and
529 juvenile villi following 30-minutes ischemia and 30-minutes *ex vivo* recovery. Note the sphering
530 and persistence of microvilli (white arrowheads) in the neonatal wound-adjacent cells (left)
531 versus the smoothed leading edges of the lamellipodia (white arrowheads) extending into the
532 remaining defect (asterisks, wound edge outlined by white dotted line) in the juveniles (right).
533 (representative of n=3, 5,000x and 10,000x, scale bars 10 μm and 3 μm)

534

535 **Figure 5. Effect of exogenous prostaglandins, full thickness *ex vivo* and *in vivo* recovery**
536 **on neonatal restitution following 30-minutes of ischemia.** (A) Representative histology of

537 control, 30-minutes ischemic and 120-minutes *ex vivo* recovery neonatal jejunum with the
538 addition of 1uM 16,16-dimethylprostaglandin E₂ to the basolateral chamber. Note the persistent
539 epithelial defect in the recovered tissue (scale bars 100 μm). (B) Histomorphometry quantified
540 74±2.5% and 68±13.3% epithelialization in injured and prostaglandin recovered tissues,
541 respectively, as compared to 98±2.0% epithelialization of controls (n=3, n.s.= not significant,
542 **P<0.01, unpaired t-test). (C) Representative histology of control, 30-minutes ischemic, and 30-
543 minutes ischemic and 120-minutes full-thickness *ex vivo* recovery neonatal jejunum (scale bars
544 100 μm). (D) Histomorphometry quantified 30±6.3% and 27±12.6% epithelialization in injured
545 and full thickness *ex vivo* recovered tissues, respectively, as compared to 100±0.0%
546 epithelialization of controls (n=4, n.s.= not significant, ****P<0.0001, unpaired t-test). (E)
547 Representative histology of control, 30-minutes ischemic, and 30-minutes ischemic and 120-
548 minutes *in vivo* recovery neonatal jejunum (scale bars 100μm). (F) Histomorphometry quantified
549 50±7.4% and 44±6.6% epithelialization in injured and *in vivo* recovered tissues, respectively,
550 versus 100% epithelialization of controls (n=5-7, n.s.= not significant, **P<0.01, unpaired t-test).

551

552 **Figure 6. Exogenous application of injured juvenile mucosal homogenate partially**

553 **rescues barrier repair in injured neonate jejunum.** (A) Application of juvenile (juv), but not
554 neonatal (neo), injured mucosal homogenate to both sides of the tissue during *ex vivo* recovery
555 rescues the TEER of ischemia-injured neonatal jejunum. Application to apical or basolateral
556 side only does not rescue TEER. Data presented is normalized relative to each individual
557 tissue's own initial TEER (n=5-6, significant effect of treatment and recovery on TEER by two-
558 way ANOVA, P≤0.001; **P<0.01, ***P<0.001 by Dunnett's multiple comparisons test). (B)
559 Representative histology shows remaining defects in neonatal homogenate-treated tissues as
560 compared to evidence of partially restituted epithelium (arrowheads) in juvenile homogenate-
561 treated tissues (n=6-12, scale bar 100μm). (C) Histomorphometry quantified 80±4.4% epithelial
562 coverage with injured juvenile mucosal homogenate on both sides of the tissue versus 40-60%

563 in all other treatment groups (n=6-12, significant effect of treatment on epithelial coverage by
564 one-way ANOVA, $P < 0.01$, $*P < 0.05$ by Dunnett's multiple comparisons test).

565

566 **Figure 7. Exogenous application of neonatal or juvenile mucosal homogenate**

567 **supernatant does not rescue barrier repair in injured neonatal jejunum.** (A) Application of
568 neither juvenile (juv) nor neonatal (neo) injured mucosal homogenate supernatant to both sides
569 of the tissue during *ex vivo* recovery can rescue the TEER of ischemia-injured neonatal
570 jejunum. Data presented is normalized relative to each individual tissue's own initial TEER (n=5;
571 significant effect of treatment but not recovery on TEER by two-way ANOVA, $P < 0.001$; no
572 significant differences versus Ringer's control by Dunnett's multiple comparisons test). (B)
573 Representative histology shows remaining defects in neonatal homogenate-treated tissues as
574 compared to evidence of partially restituted epithelium (arrowheads) in juvenile homogenate-
575 treated tissues (n=6-12; scale bar 100 μ m). (C) Histomorphometry quantified $70 \pm 8.4\%$ epithelial
576 coverage in Ringer's recovered tissue which did not differ from epithelial coverage in
577 supernatant treated groups ($61 \pm 11.0\%$ and $71 \pm 11.3\%$ for neonate and juvenile, respectively)
578 (n=5-6; no differences by one-way ANOVA).

579

580 **Supplemental Figure 1. Injury induced similar PGE₂ production in the jejunum of**

581 **neonates and juveniles.** PGE₂ production in the basolateral Ringer's solution at 60-minutes of
582 *ex vivo* recovery was induced by ischemic injury similarly across both age groups. (n=5;
583 $P < 0.001$ for effect of injury on PGE₂ by two-way ANOVA; n.s. = no significant difference on
584 Sidak's multiple comparisons test).

585

586 **FUNDING**

587 Supported by funding from UNC CGIBD Large Animal Models Core (P30 DK034987)

588 UNC CGIBD Basic Science Research Training Fellowship (NIH T32 5T32DK007737-22), USDA
589 National Institute of Food and Agriculture, Animal Health (Project 1007263), an intramural NC
590 State CMI TPP Seed Grant (2017), and an NC State College of Veterinary Medicine Intramural
591 Grant (2017).

592

593 **COMPETING INTERESTS**

594 The authors have no competing interests to declare.

595

596 **REFERENCES**

- 597 1. Blikslager AT, Moeser AJ, Gookin JL, Jones SL, Odle J. Restoration of barrier function in
598 injured intestinal mucosa. *Physiol Rev.* 2007;87(2):545-64.
- 599 2. Young CM, Kingma SD, Neu J. Ischemia-reperfusion and neonatal intestinal injury. *The*
600 *Journal of pediatrics.* 2011;158(2 Suppl):e25-8.
- 601 3. Fitzgibbons SC, Ching Y, Yu D, Carpenter J, Kenny M, Weldon C, et al. Mortality of
602 necrotizing enterocolitis expressed by birth weight categories. *Journal of pediatric surgery.*
603 2009;44(6):1072-5; discussion 5-6.
- 604 4. Watkins DJ, Besner GE. The role of the intestinal microcirculation in necrotizing
605 enterocolitis. *Semin Pediatr Surg.* 2013;22(2):83-7.
- 606 5. Neu J, Walker WA. Necrotizing enterocolitis. *The New England journal of medicine.*
607 2011;364(3):255-64.
- 608 6. Mammen JM, Matthews JB. Mucosal repair in the gastrointestinal tract. *Critical care*
609 *medicine.* 2003;31(8 Suppl):S532-7.
- 610 7. Kirk AD. Crossing the bridge: large animal models in translational transplantation
611 research. *Immunological reviews.* 2003;196:176-96.
- 612 8. Swindle MM, Makin A, Herron AJ, Clubb FJ, Jr., Frazier KS. Swine as models in
613 biomedical research and toxicology testing. *Veterinary pathology.* 2012;49(2):344-56.
- 614 9. Roura E KS, Lallès JP, Le Huerou-Luron, de Jager N, Schuurman T, Val-Laillet D.
615 Critical review evaluating the pig as a model for human nutritional physiology. *Nutritional*
616 *Research Reviews.* 2016;29(1):60-90.
- 617 10. Rothkotter HJ, Sowa E, Pabst R. The pig as a model of developmental immunology.
618 *Human & experimental toxicology.* 2002;21(9-10):533-6.
- 619 11. Bendixen E, Danielsen M, Larsen K, Bendixen C. Advances in porcine genomics and
620 proteomics--a toolbox for developing the pig as a model organism for molecular biomedical
621 research. *Briefings in functional genomics.* 2010;9(3):208-19.

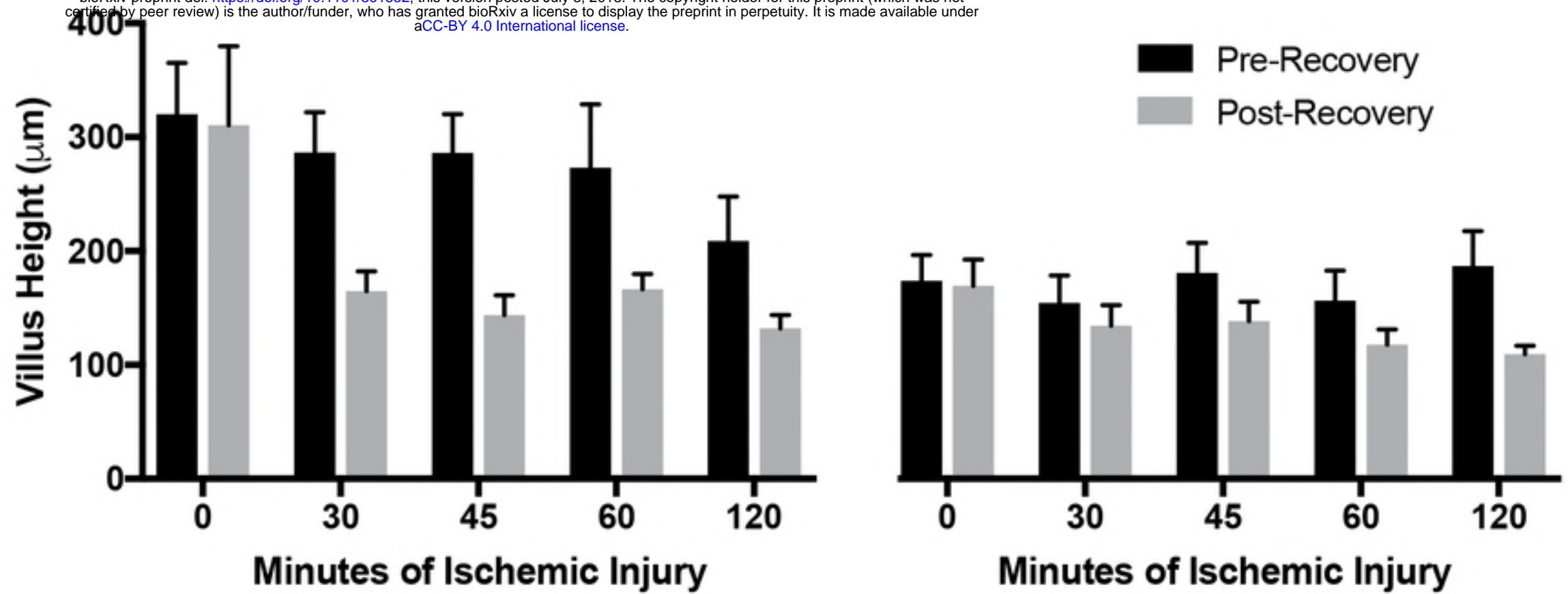
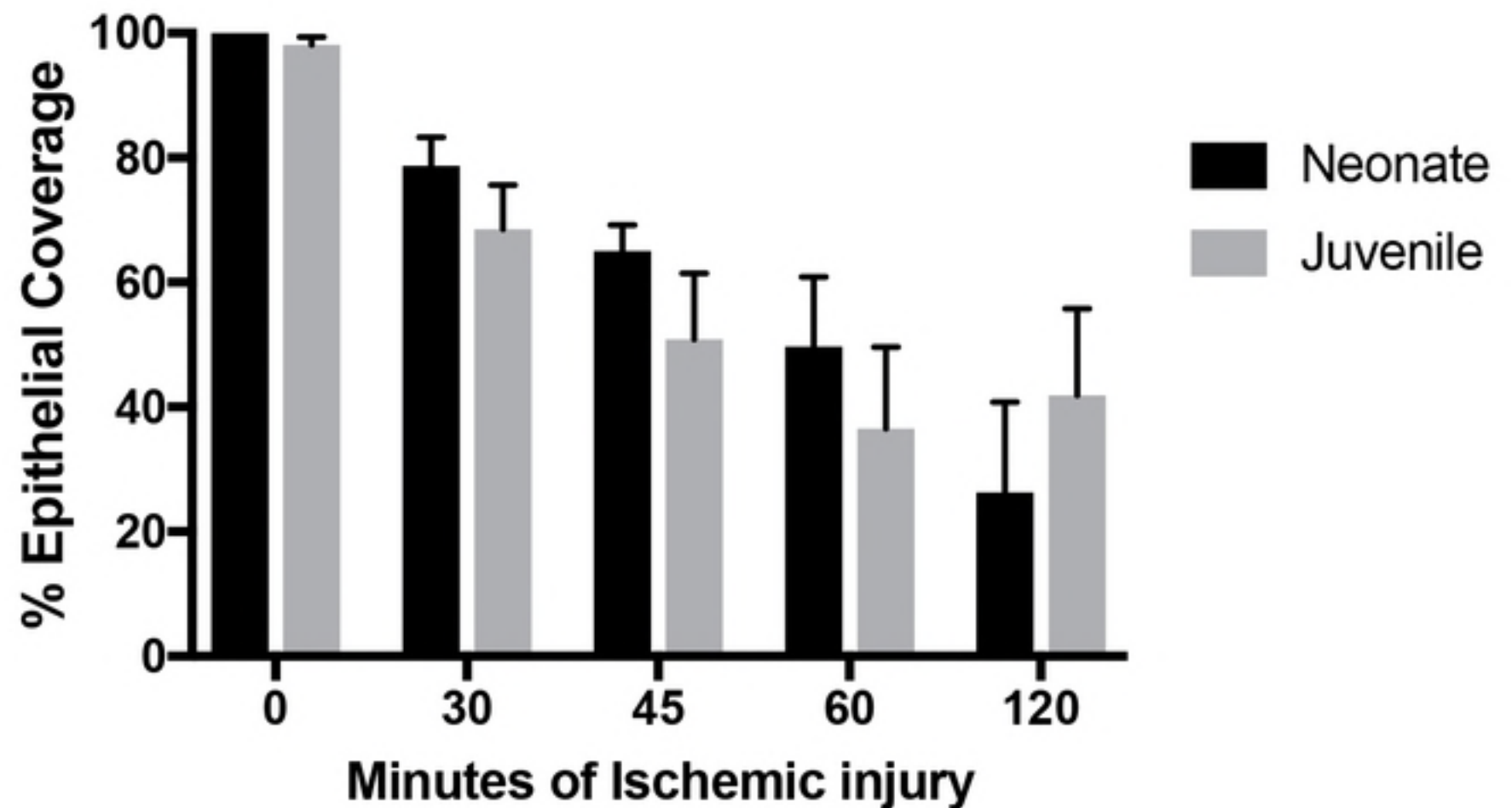
- 622 12. Lunney JK. Advances in swine biomedical model genomics. *International journal of*
623 *biological sciences*. 2007;3(3):179-84.
- 624 13. Hart EA, Caccamo M, Harrow JL, Humphray SJ, Gilbert JG, Trevanion S, et al. Lessons
625 learned from the initial sequencing of the pig genome: comparative analysis of an 8 Mb region
626 of pig chromosome 17. *Genome biology*. 2007;8(8):R168.
- 627 14. Ibrahim Z, Busch J, Awwad M, Wagner R, Wells K, Cooper DK. Selected physiologic
628 compatibilities and incompatibilities between human and porcine organ systems.
629 *Xenotransplantation*. 2006;13(6):488-99.
- 630 15. Ziegler A, Gonzalez L, Blikslager A. Large Animal Models: The Key to Translational
631 Discovery in Digestive Disease Research. *Cell Mol Gastroenterol Hepatol*. 2016;2(6):716-24.
- 632 16. Jacobi SK, Moeser AJ, Corl BA, Harrell RJ, Blikslager AT, Odle J. Dietary long-chain
633 PUFA enhance acute repair of ischemia-injured intestine of suckling pigs. *The Journal of*
634 *nutrition*. 2012;142(7):1266-71.
- 635 17. Moeser AJ, Nighot PK, Engelke KJ, Ueno R, Blikslager AT. Recovery of mucosal barrier
636 function in ischemic porcine ileum and colon is stimulated by a novel agonist of the ClC-2
637 chloride channel, lubiprostone. *Am J Physiol Gastrointest Liver Physiol*. 2007;292(2):G647-56.
- 638 18. Argenzio RA, Lecce J, Powell DW. Prostanoids inhibit intestinal NaCl absorption in
639 experimental porcine cryptosporidiosis. *Gastroenterology*. 1993;104(2):440-7.
- 640 19. Derikx JP, Matthijsen RA, de Bruine AP, van Bijnen AA, Heineman E, van Dam RM, et
641 al. Rapid reversal of human intestinal ischemia-reperfusion induced damage by shedding of
642 injured enterocytes and reepithelialisation. *PLoS One*. 2008;3(10):e3428.
- 643 20. Pelsers MM, Hermens WT, Glatz JF. Fatty acid-binding proteins as plasma markers of
644 tissue injury. *Clinica chimica acta; international journal of clinical chemistry*. 2005;352(1-2):15-
645 35.

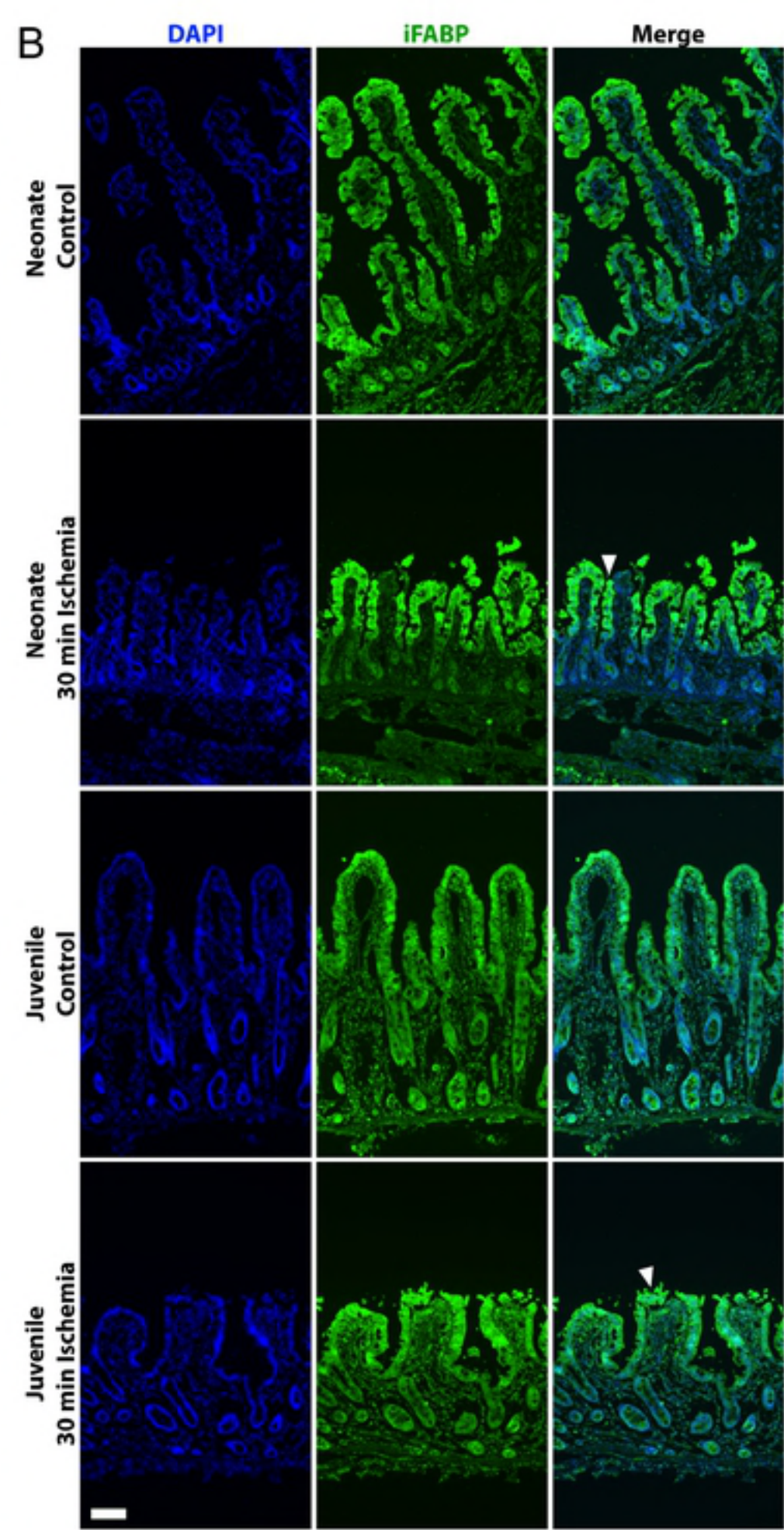
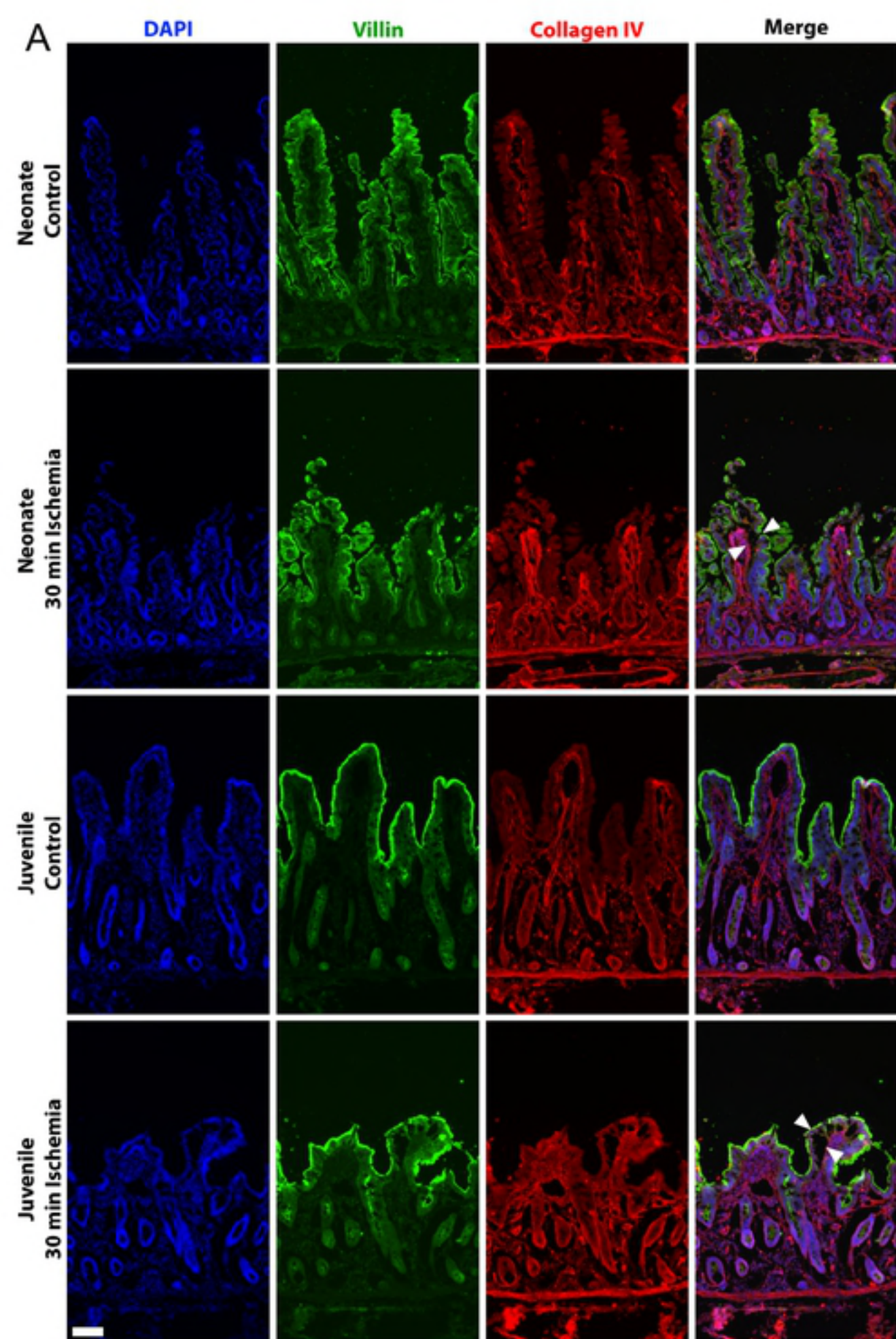
- 646 21. Schellekens DH, Hundscheid IH, Leenarts CA, Grootjans J, Lenaerts K, Buurman WA,
647 et al. Human small intestine is capable of restoring barrier function after short ischemic periods.
648 World journal of gastroenterology : WJG. 2017;23(48):8452-64.
- 649 22. Gonzalez LM, Moeser AJ, Blikslager AT. Animal models of ischemia-reperfusion-
650 induced intestinal injury: progress and promise for translational research. Am J Physiol
651 Gastrointest Liver Physiol. 2015;308(2):G63-75.
- 652 23. Gonzalez LM, Williamson I, Piedrahita JA, Blikslager AT, Magness ST. Cell lineage
653 identification and stem cell culture in a porcine model for the study of intestinal epithelial
654 regeneration. PLoS One. 2013;8(6):e66465.
- 655 24. Mahoney ZX, Stappenbeck TS, Miner JH. Laminin alpha 5 influences the architecture of
656 the mouse small intestine mucosa. Journal of cell science. 2008;121(Pt 15):2493-502.
- 657 25. Lefebvre O, Sorokin L, Kedinger M, Simon-Assmann P. Developmental expression and
658 cellular origin of the laminin alpha2, alpha4, and alpha5 chains in the intestine. Developmental
659 biology. 1999;210(1):135-50.
- 660 26. Blikslager AT, Roberts MC, Rhoads JM, Argenzio RA. Prostaglandins I2 and E2 have a
661 synergistic role in rescuing epithelial barrier function in porcine ileum. The Journal of clinical
662 investigation. 1997;100(8):1928-33.
- 663 27. Blikslager AT, Malcolm C. Roberts, Robert A. Argenzio. Prostaglandin-induced recovery
664 of barrier function in porcine ileum is triggered by chloride secretion. American Journal of
665 Physiology 1999;276:G28–G36.
- 666 28. Van Landeghem L, Chevalier J, Mahe MM, Wedel T, Urvil P, Derkinderen P, et al.
667 Enteric glia promote intestinal mucosal healing via activation of focal adhesion kinase and
668 release of proEGF. Am J Physiol Gastrointest Liver Physiol. 2011;300(6):G976-87.
- 669 29. Savidge TC, Newman P, Pothoulakis C, Ruhl A, Neunlist M, Bourreille A, et al. Enteric
670 glia regulate intestinal barrier function and inflammation via release of S-nitrosoglutathione.
671 Gastroenterology. 2007;132(4):1344-58.

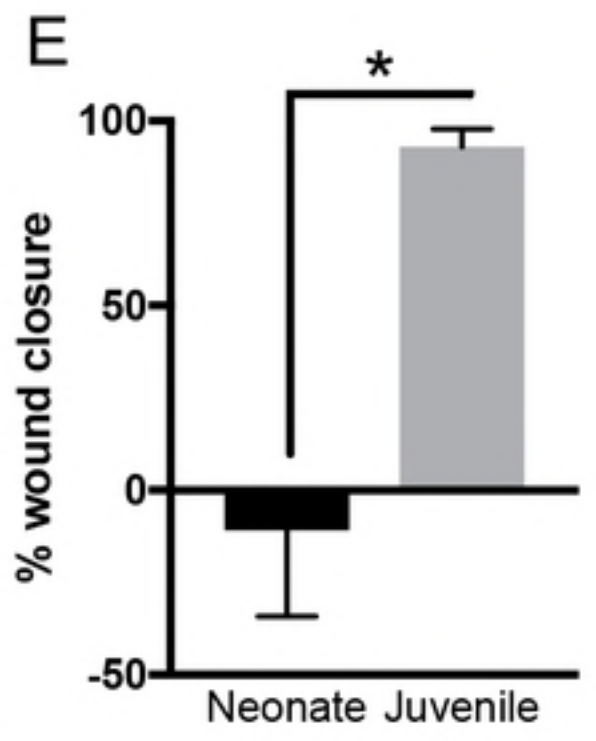
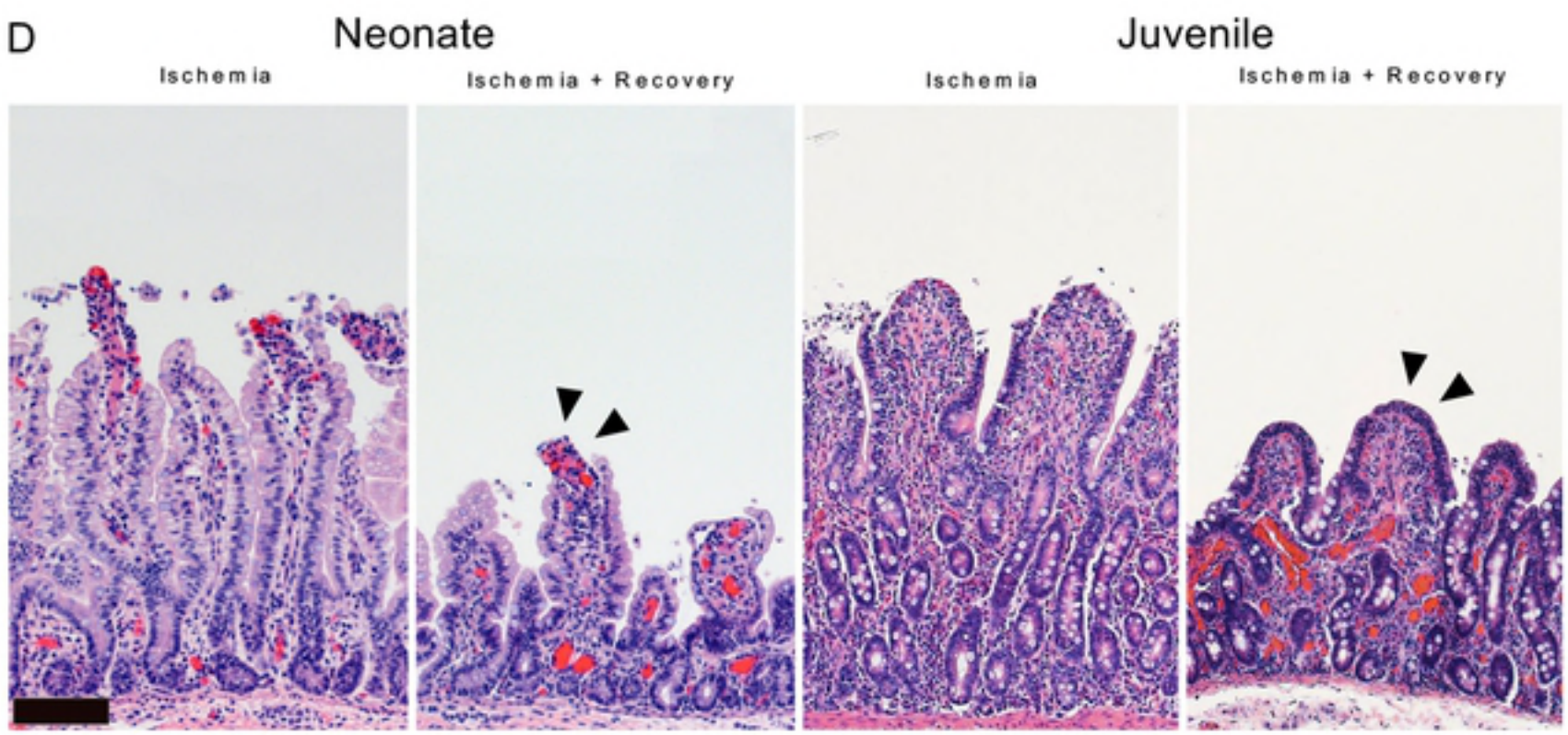
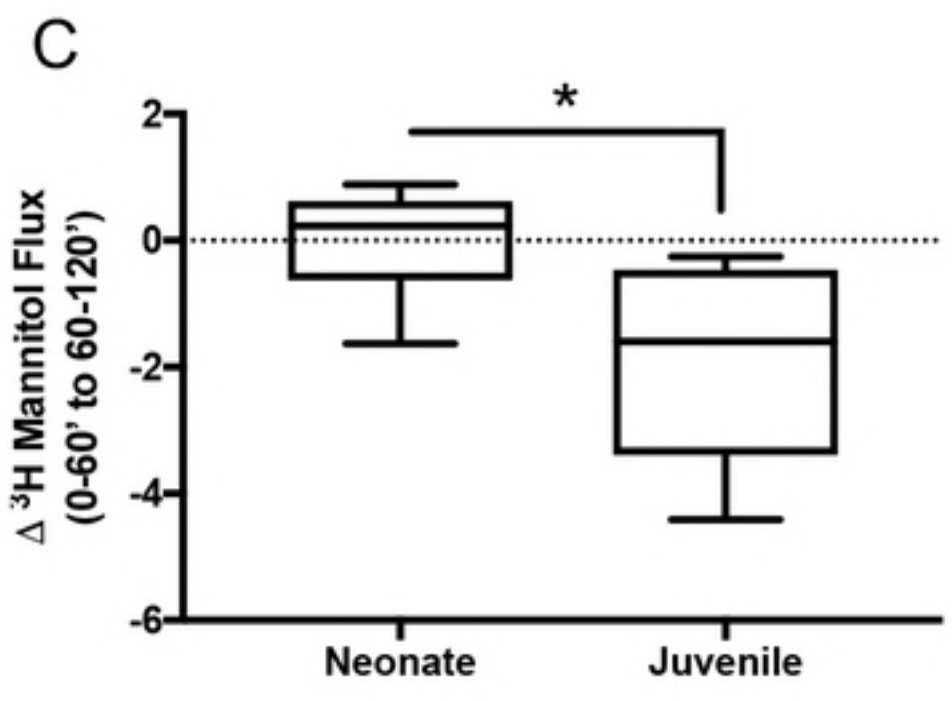
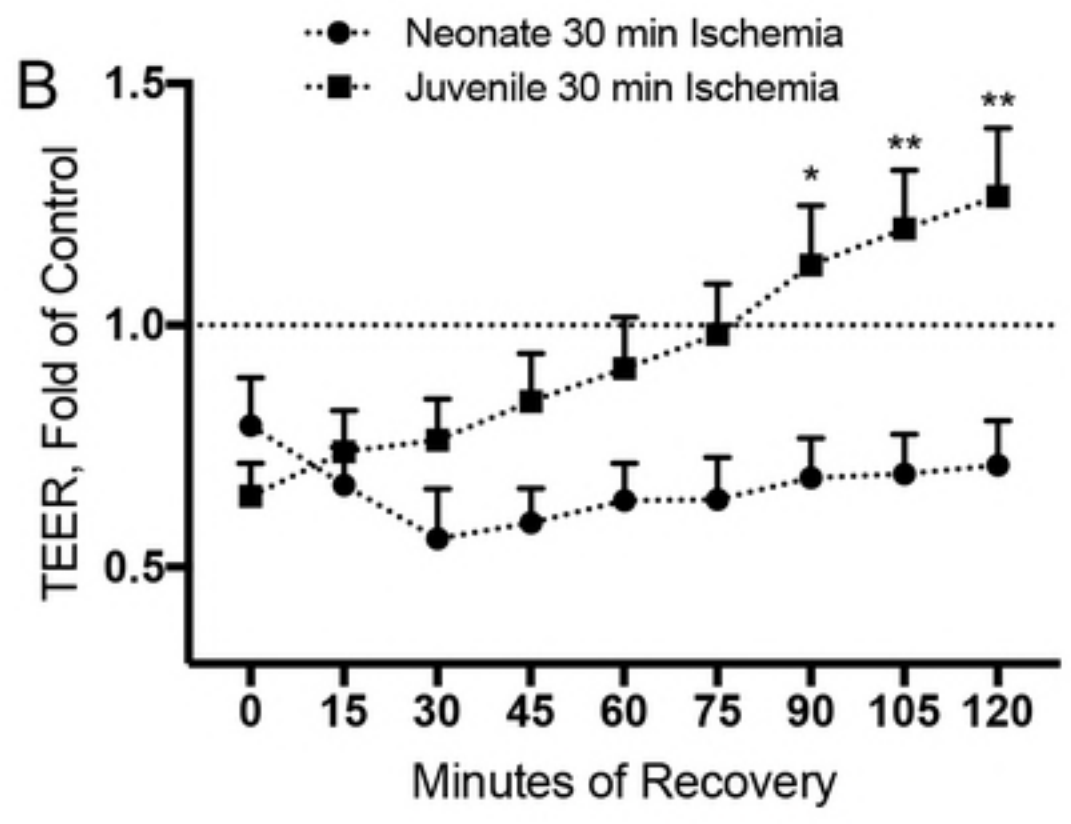
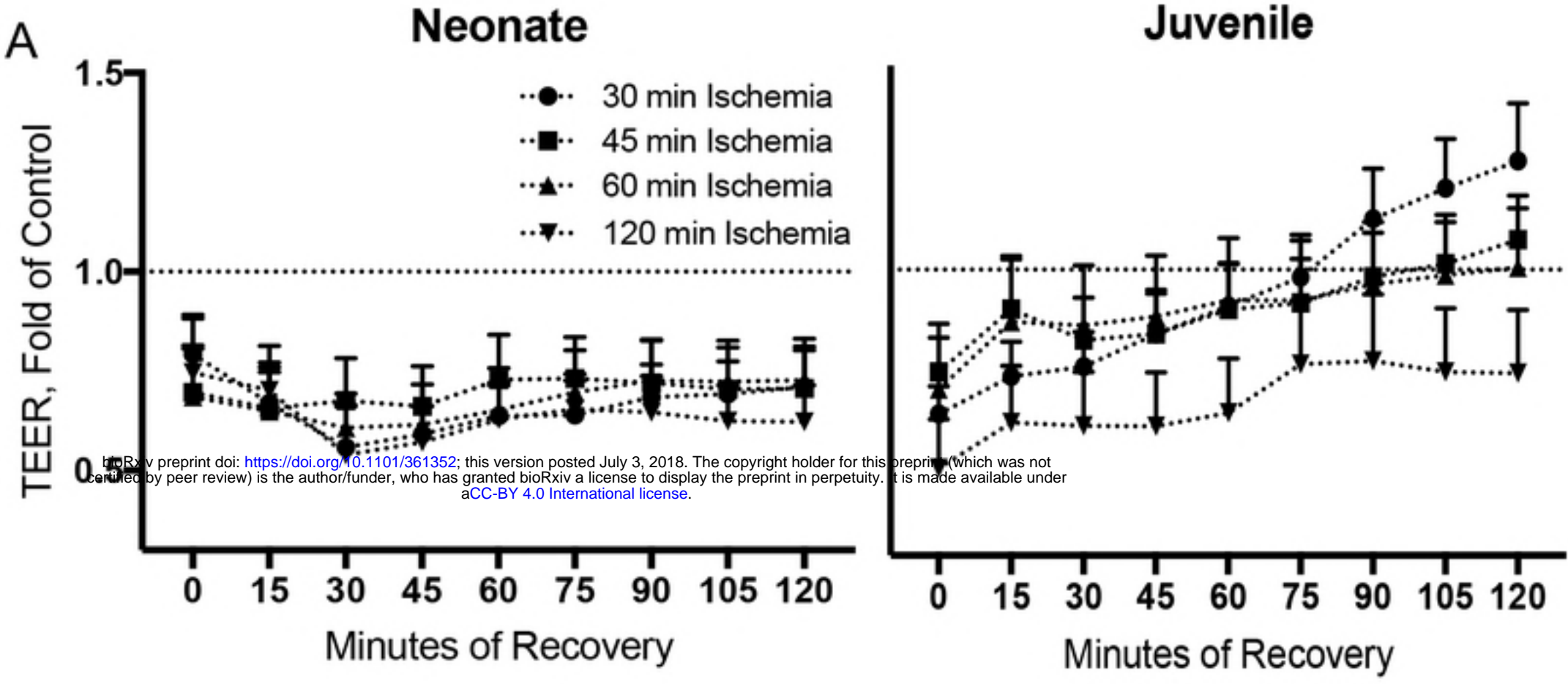
- 672 30. Coquenlorge S, Van Landeghem L, Jaulin J, Cenac N, Vergnolle N, Duchalais E, et al.
673 The arachidonic acid metabolite 11beta-ProstaglandinF2alpha controls intestinal epithelial
674 healing: deficiency in patients with Crohn's disease. *Scientific reports*. 2016;6:25203.
- 675 31. Xiao W, Wang W, Chen W, Sun L, Li X, Zhang C, et al. GDNF is involved in the barrier-
676 inducing effect of enteric glial cells on intestinal epithelial cells under acute ischemia reperfusion
677 stimulation. *Molecular neurobiology*. 2014;50(2):274-89.
- 678 32. Cossais F, Durand T, Chevalier J, Boudaud M, Kermarrec L, Aubert P, et al. Postnatal
679 development of the myenteric glial network and its modulation by butyrate. *Am J Physiol*
680 *Gastrointest Liver Physiol*. 2016;310(11):G941-51.
- 681 33. Neunlist M, Aubert P, Bonnaud S, Van Landeghem L, Coron E, Wedel T, et al. Enteric
682 glia inhibit intestinal epithelial cell proliferation partly through a TGF-beta1-dependent pathway.
683 *Am J Physiol Gastrointest Liver Physiol*. 2007;292(1):G231-41.
- 684 34. Kabouridis PS, Lasrado R, McCallum S, Chng SH, Snippert HJ, Clevers H, et al.
685 Microbiota controls the homeostasis of glial cells in the gut lamina propria. *Neuron*.
686 2015;85(2):289-95.
- 687

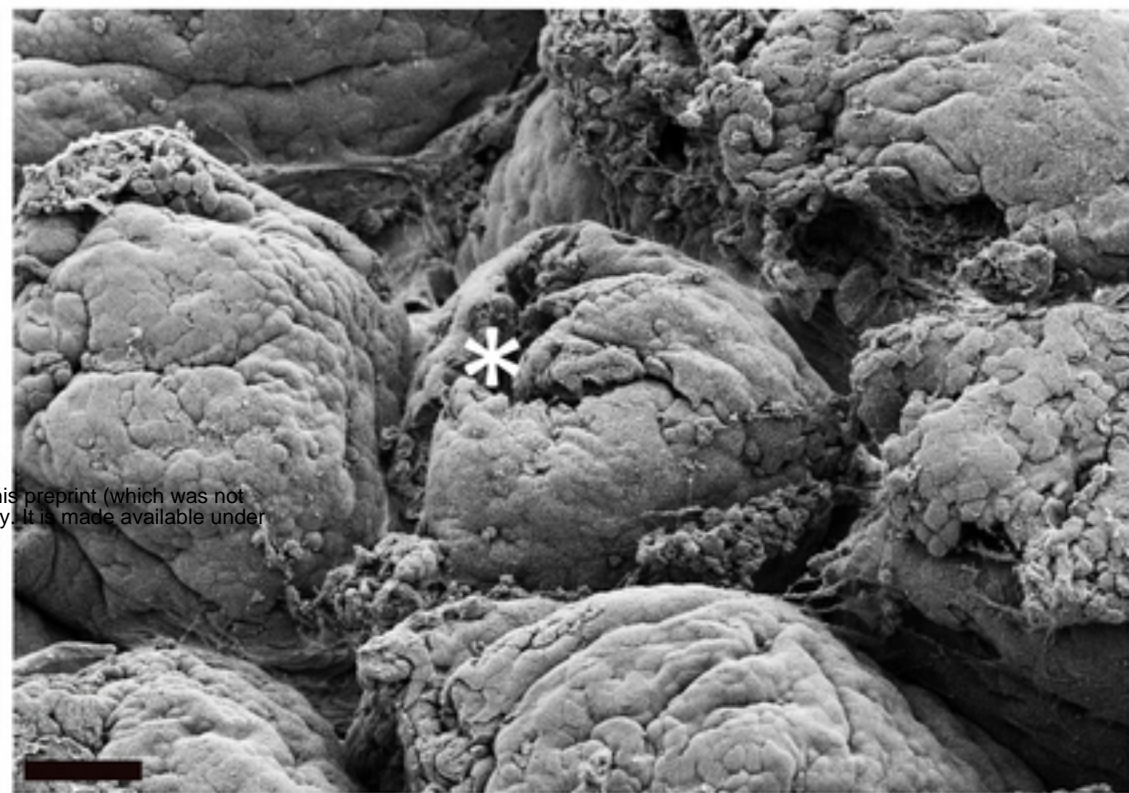
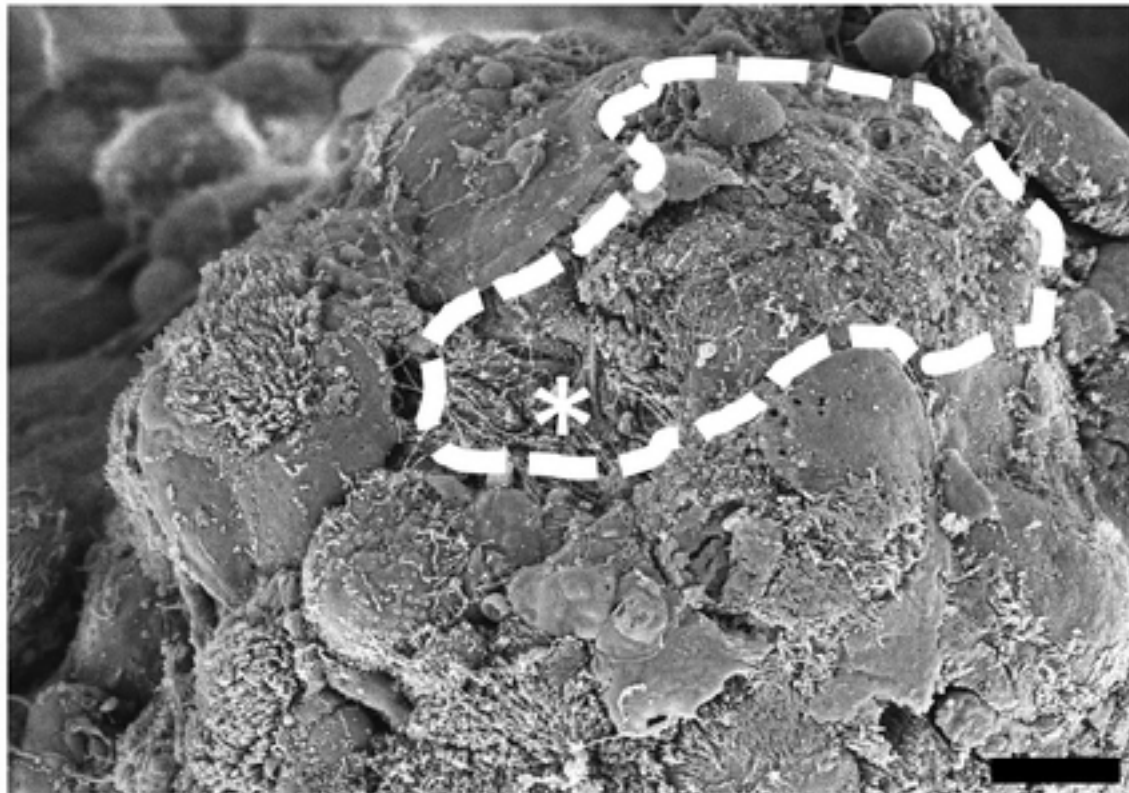
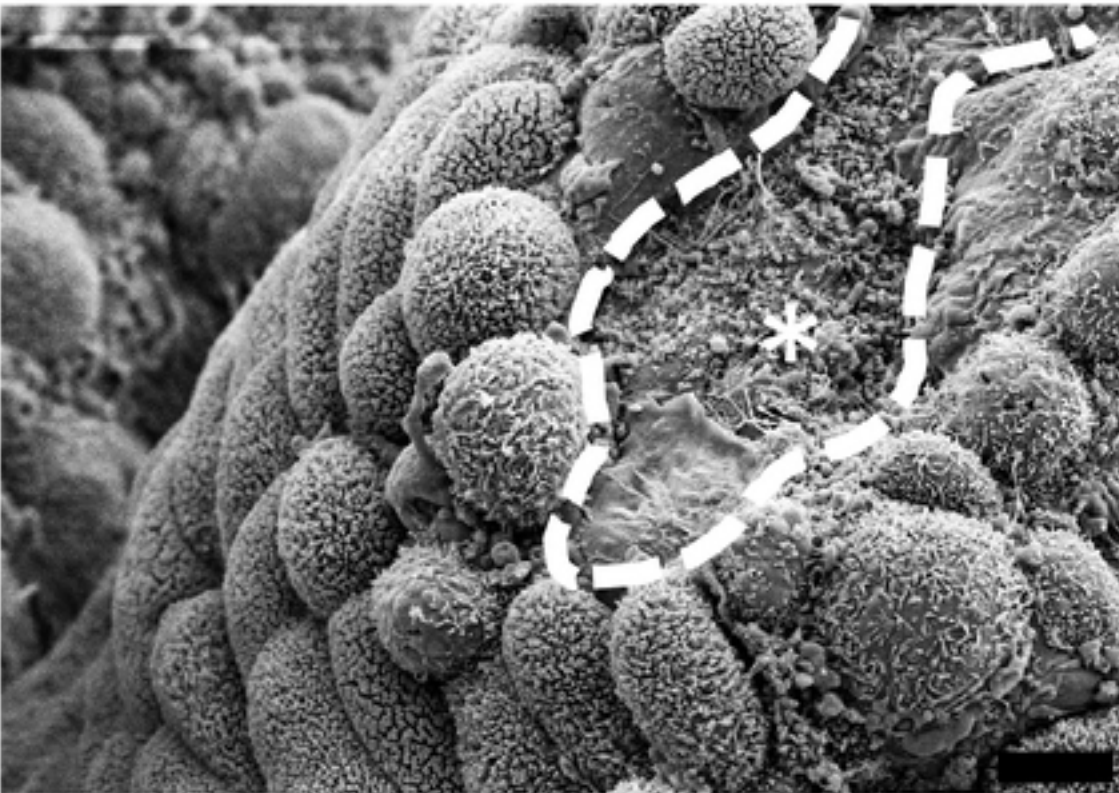
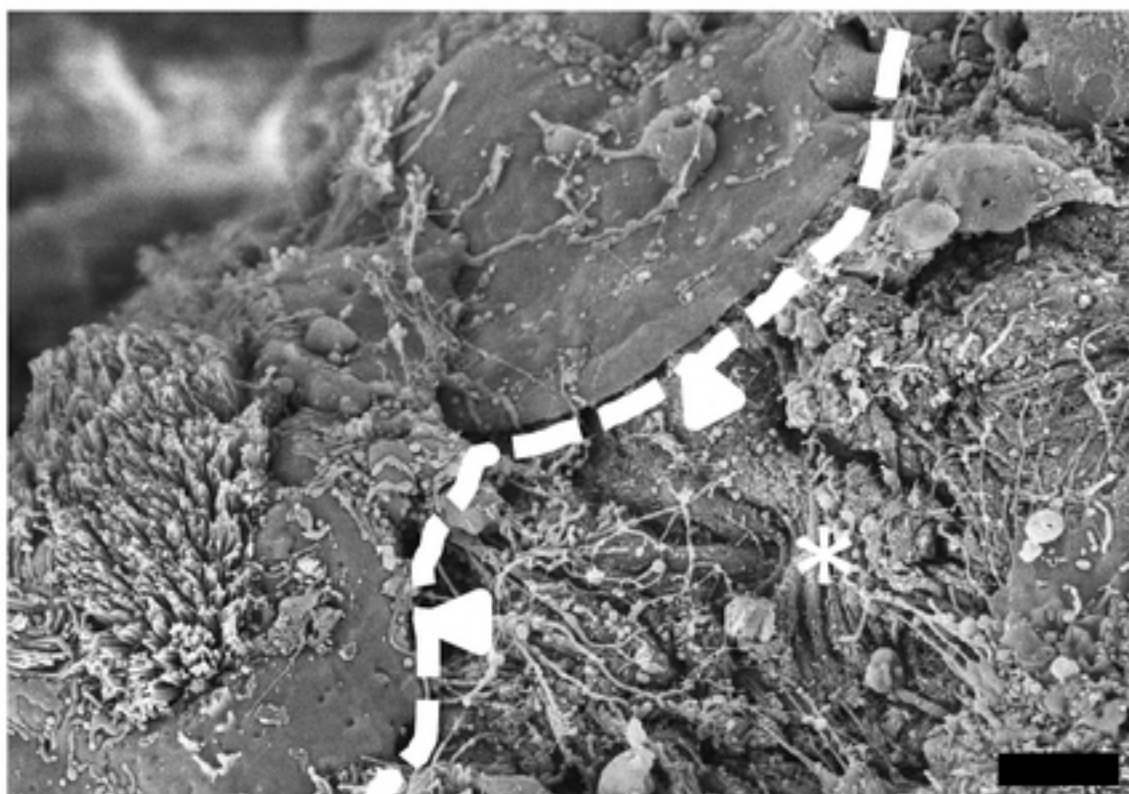
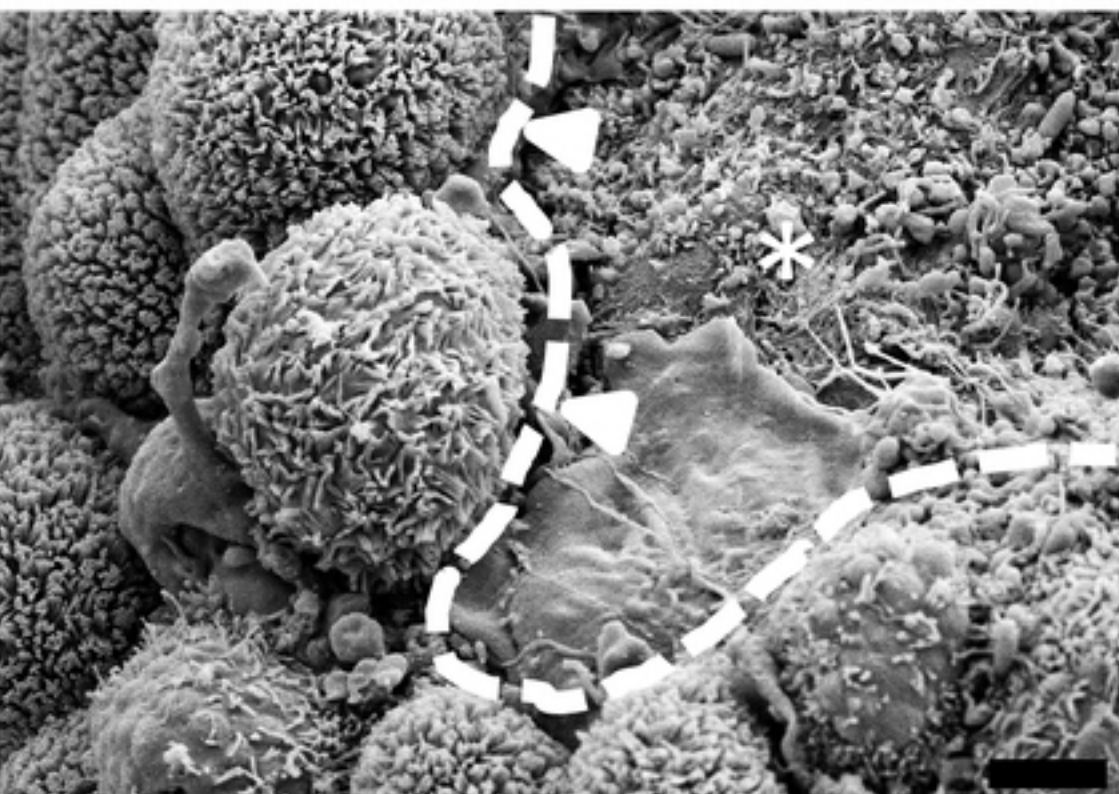
A**Neonate****Juvenile**

bioRxiv preprint doi: <https://doi.org/10.1101/361352>; this version posted July 3, 2018. The copyright holder for this preprint (which was not certified by peer review) is the author/funder, who has granted bioRxiv a license to display the preprint in perpetuity. It is made available under aCC-BY 4.0 International license.

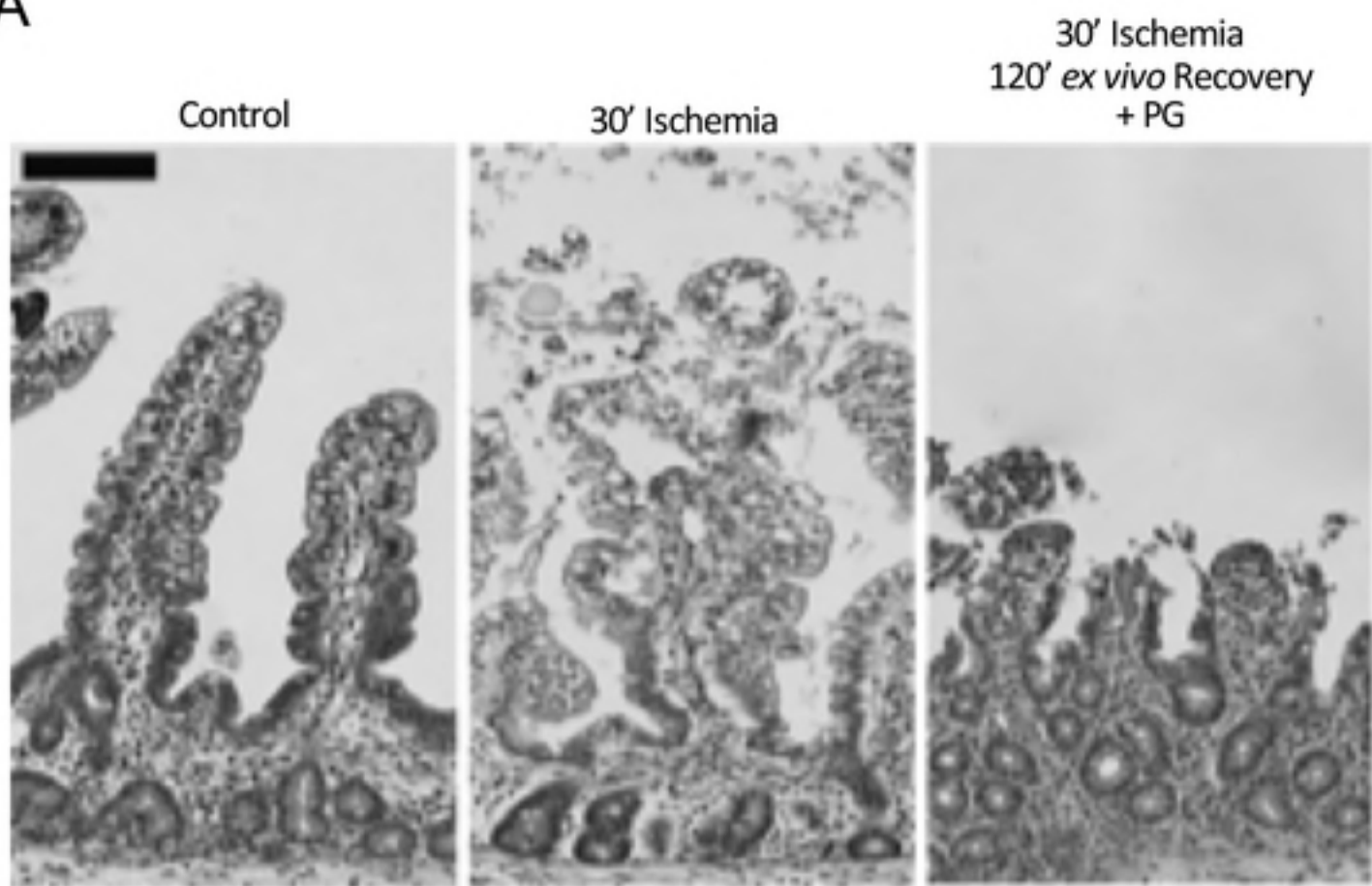
**B**





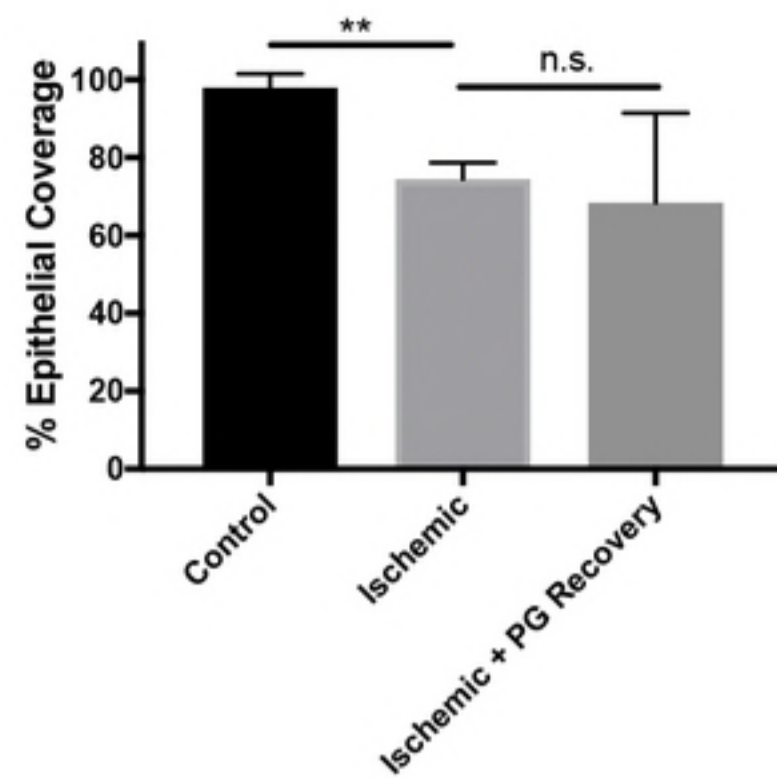
A**Neonate****Juvenile****1,000x magnification****B****Neonate****Juvenile****5,000x magnification****10,000x magnification**

A

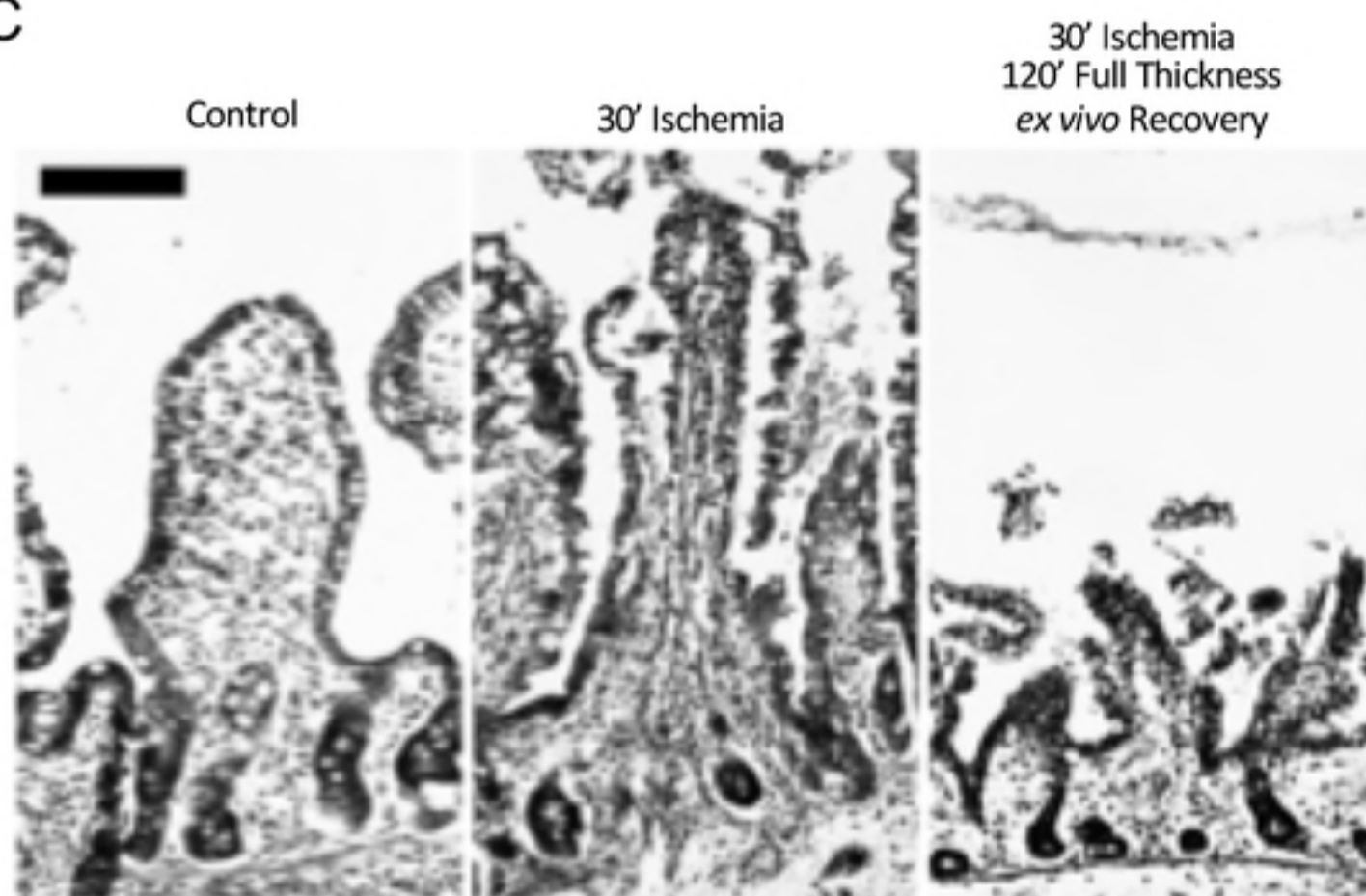


bioRxiv preprint doi: <https://doi.org/10.1101/361352>; this version posted July 3, 2018. The copyright holder for this preprint (which was not certified by peer review) is the author/funder, who has granted bioRxiv a license to display the preprint in perpetuity. It is made available under aCC-BY 4.0 International license.

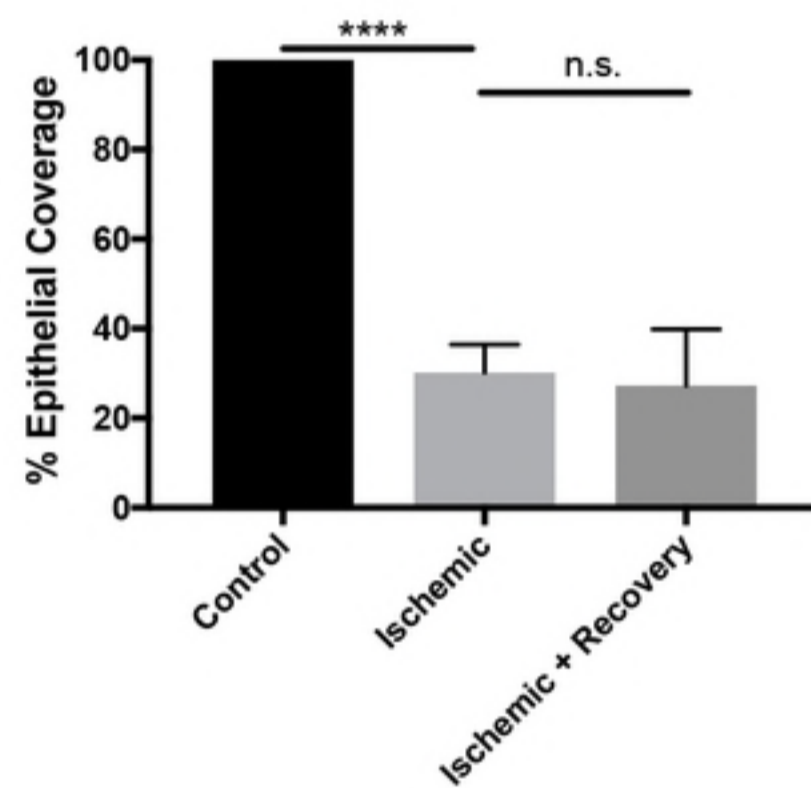
B



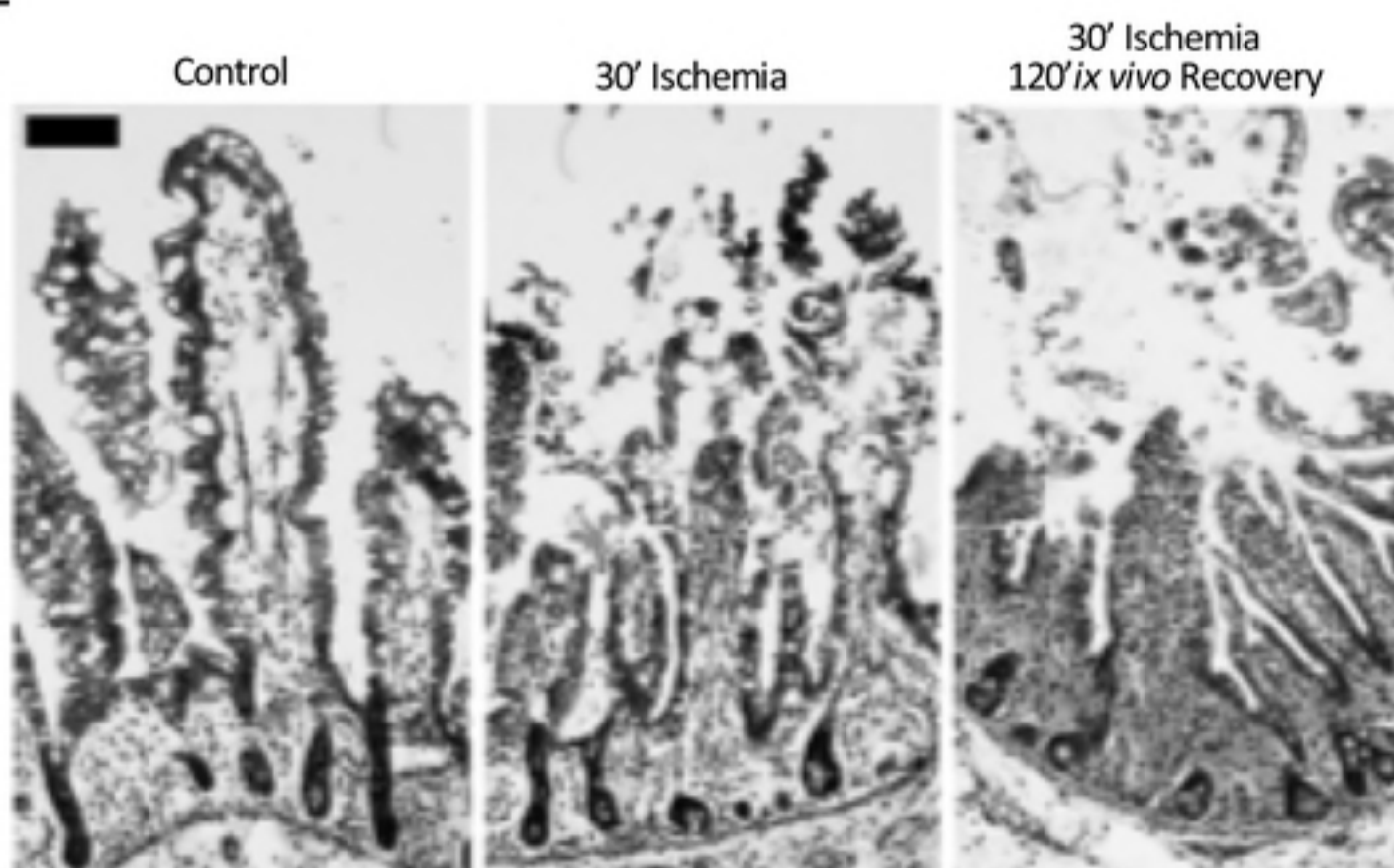
C



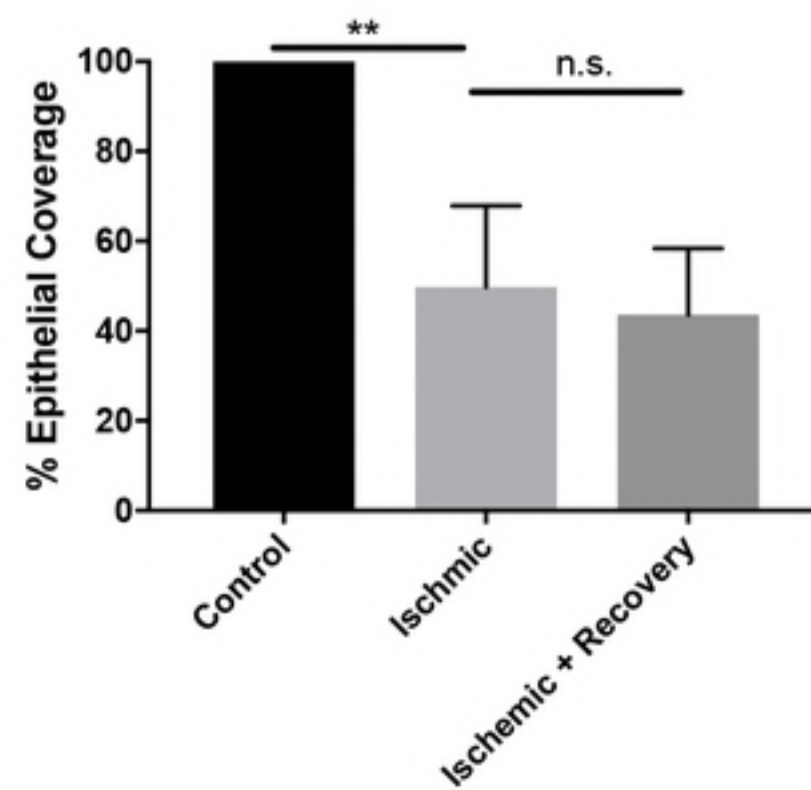
D

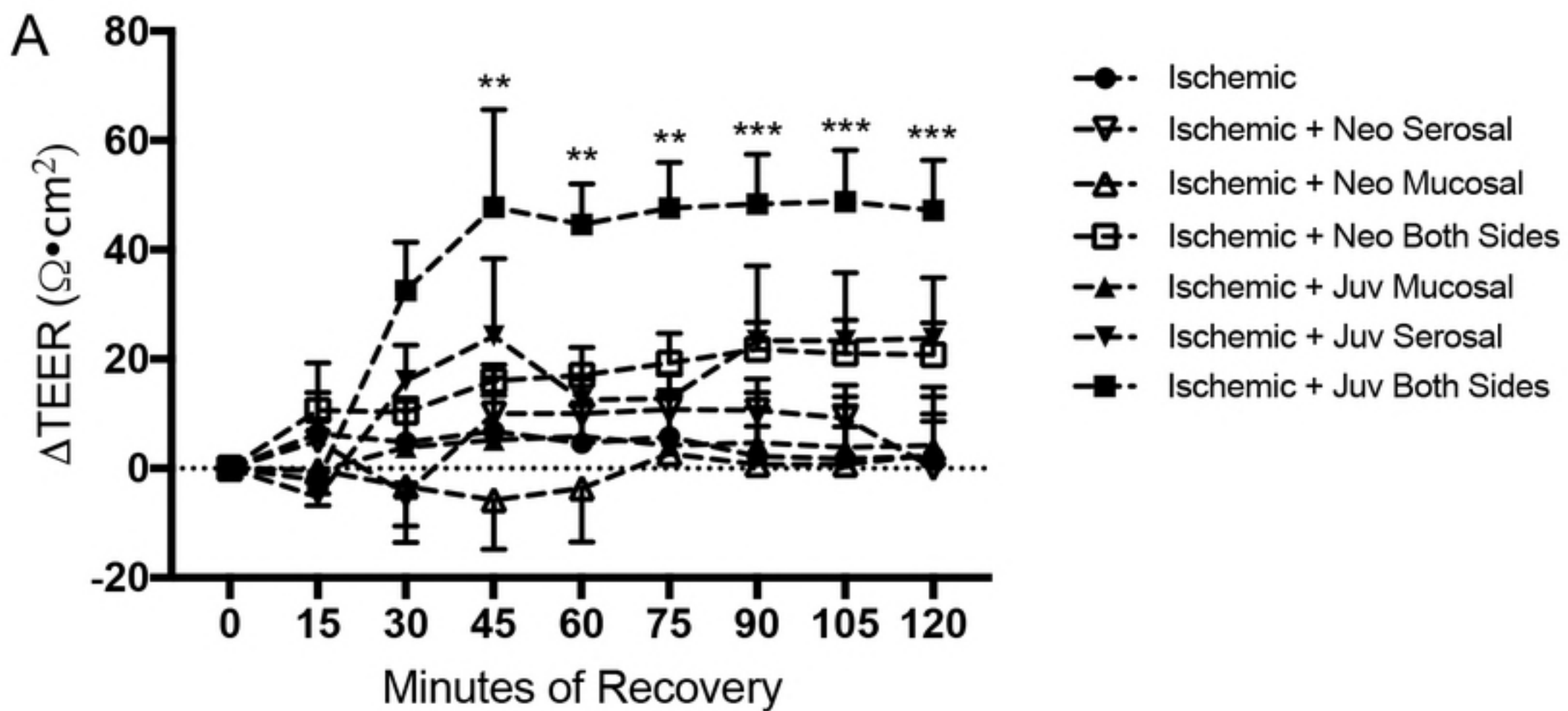


E

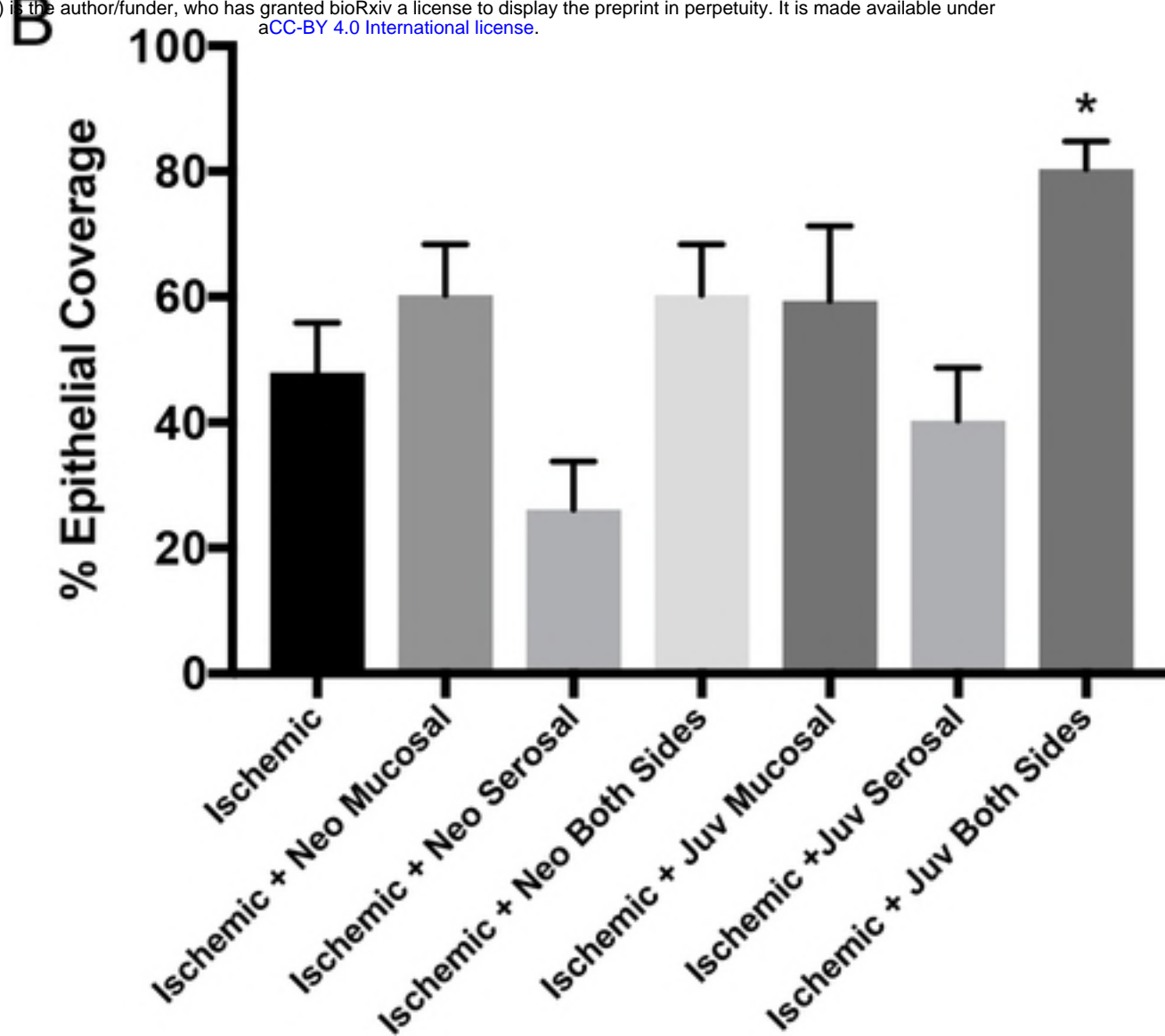


F

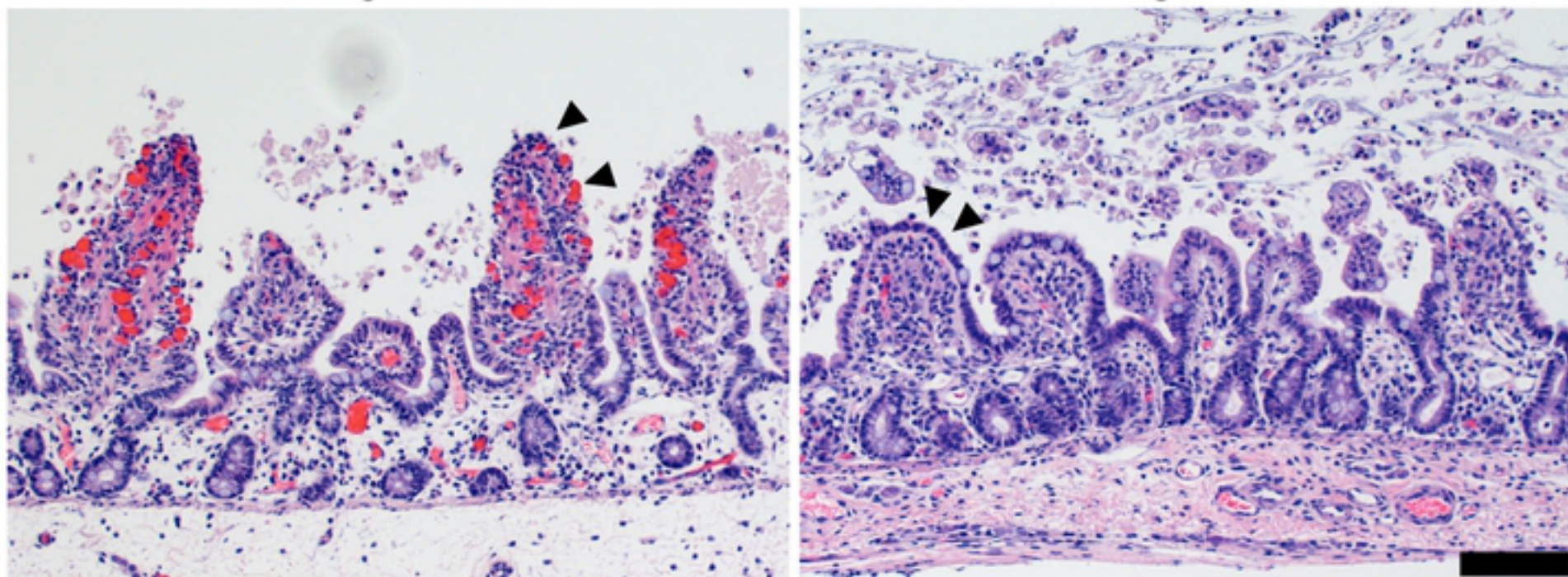


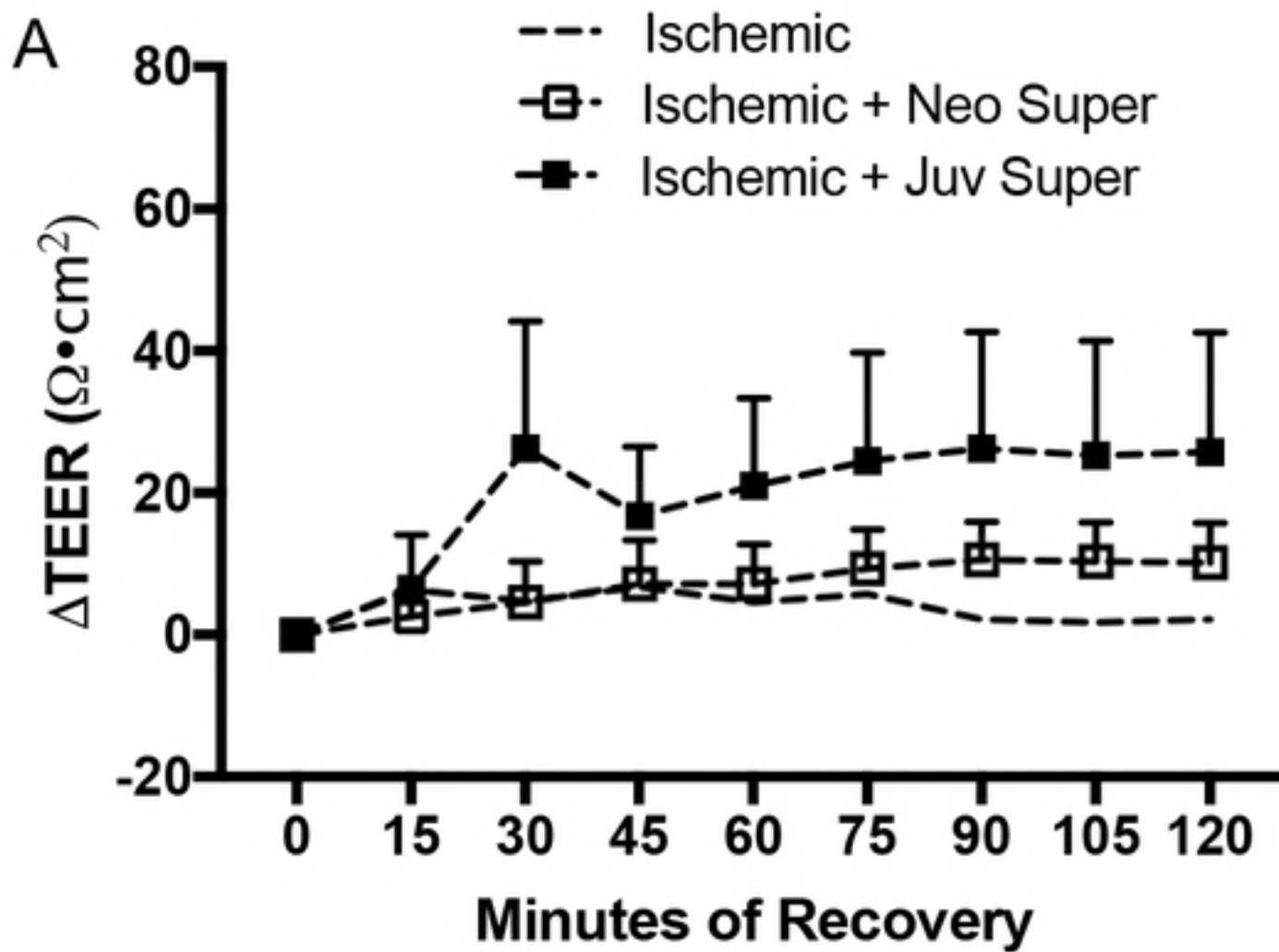


bioRxiv preprint doi: <https://doi.org/10.1101/361352>; this version posted July 3, 2018. The copyright holder for this preprint (which was not certified by peer review) is the author/funder, who has granted bioRxiv a license to display the preprint in perpetuity. It is made available under aCC-BY 4.0 International license.



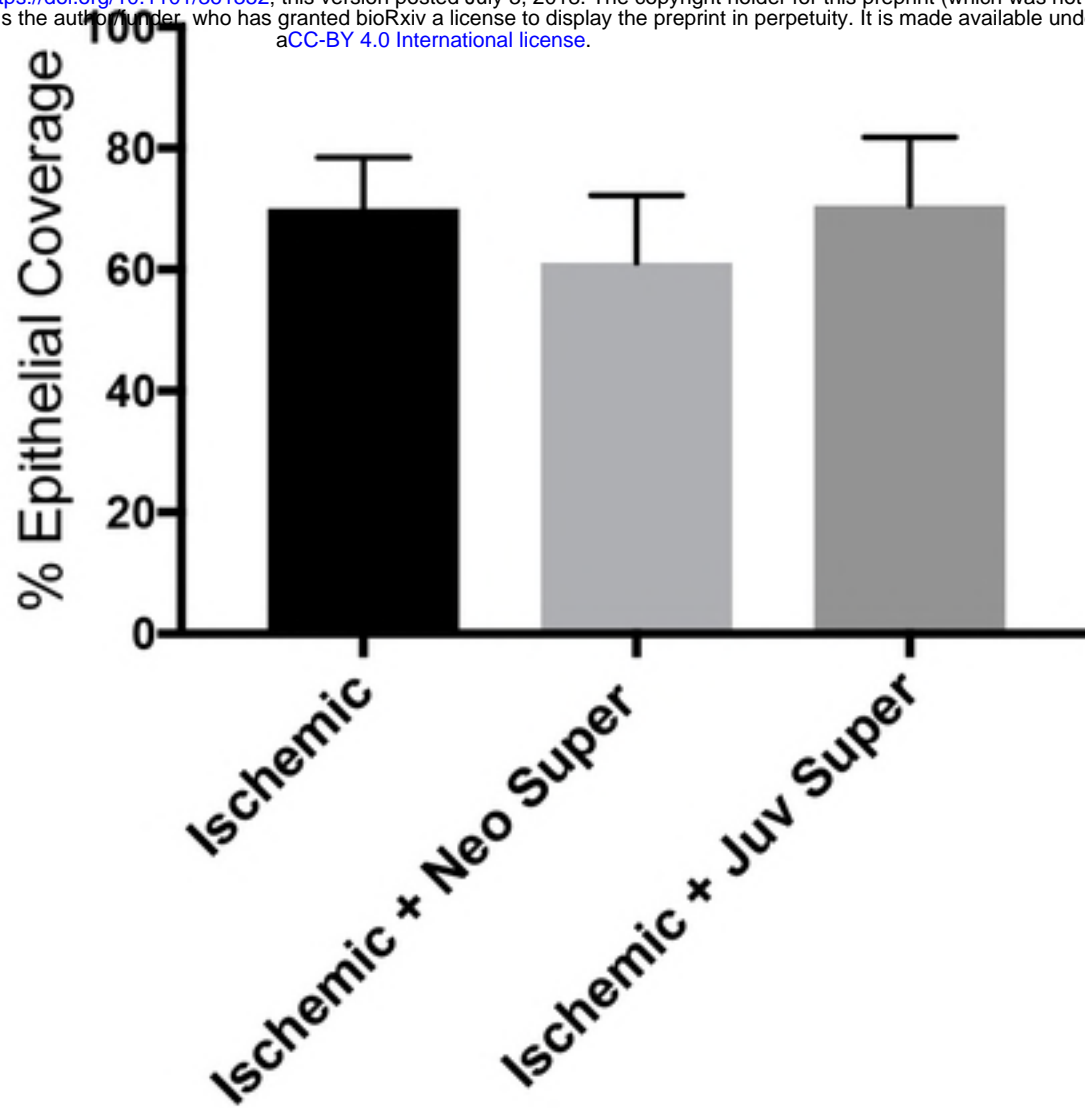
C Neonate Homogenate, Both Sides Juvenile Homogenate, Both Sides





B

bioRxiv preprint doi: <https://doi.org/10.1101/361352>; this version posted July 3, 2018. The copyright holder for this preprint (which was not certified by peer review) is the author/funder, who has granted bioRxiv a license to display the preprint in perpetuity. It is made available under aCC-BY 4.0 International license.



C

Neonate Supernatant

Juvenile Supernatant

